

# First Steps Toward the Automatic Registration of Deformable Scans

Hao Li and Mark Pauly





## Abstract

Three-dimensional registration is the process of aligning scans of different incomplete views of an object such that their corresponding regions agree in space and time. It is used to build digital complete models from partial acquisitions of real-world objects which typically contain noise, outliers, and acquisition holes due to occlusions and hardware limitations. For non-rigid models, such as humans, shapes of corresponding regions undergo complex deformations in addition to misalignments. Thus, finding explicit correspondences between two dissimilar shapes becomes considerably more challenging. In addition, finding the right deformations is also non-trivial as they depend on the correspondences which are only partially available between consecutive scans.

This report presents an analysis of the 3-D registration problem, a general approach for the spatio-temporal registration of deformable scans that are acquired with a fast 3-D scanner, and extensive experiments on synthetic and real acquisition data. The objective is to un-deform the surfaces of all range maps and to fit them into a particular instance of time.

We address this problem by finding point correspondences based on initial closest point computations between partial scans and performing deformations according to these matches. Similar to the *iterative closest point* (ICP) algorithm, the correspondence and deformation steps are tightly coupled and optimized within a loop. Although smooth and small scale deformations between consecutive scans are assumed, we envision allowing large deformations, such as human bodies in completely different poses, during the acquisition. This approach is the main distinction over previous work on non-rigid ICP variants, where the accumulation of registration errors has to be globally minimized. The suggested approach makes extensive use of assumptions on surface and deformation smoothness.

Our experiments confirm the success of our method for small deformations where the error accumulation of the correspondences over time is limited. However, this preliminary investigation shows that without additional assumptions about the correspondence flow and object deformation, such as rigidity and near-isometry, registration of scans with large scale deformations remains an unsolved problem. Nevertheless, promising intermediate results open up a new line of sub-problems needed to be solved for the grand challenge of fully automatic reconstruction of surface, motion, and correspondence from time coherent range-scans.



# Contents

<b>1</b>	<b>Introduction</b>	<b>1</b>
1.1	Previous Work . . . . .	5
1.2	Assumptions Analysis . . . . .	8
<b>2</b>	<b>Spatio-temporal Registration</b>	<b>11</b>
2.1	A General Framework . . . . .	11
2.2	Pairwise Correspondence . . . . .	17
2.3	Deformation Model . . . . .	21
<b>3</b>	<b>Preliminary Results</b>	<b>27</b>
3.1	Experiments . . . . .	27
3.2	Caveats and Implications . . . . .	33
<b>4</b>	<b>Summary and Outlook</b>	<b>37</b>
4.1	Research Status . . . . .	37
4.2	Future Directions . . . . .	38
	<b>Bibliography</b>	<b>45</b>



# Chapter 1

## Introduction

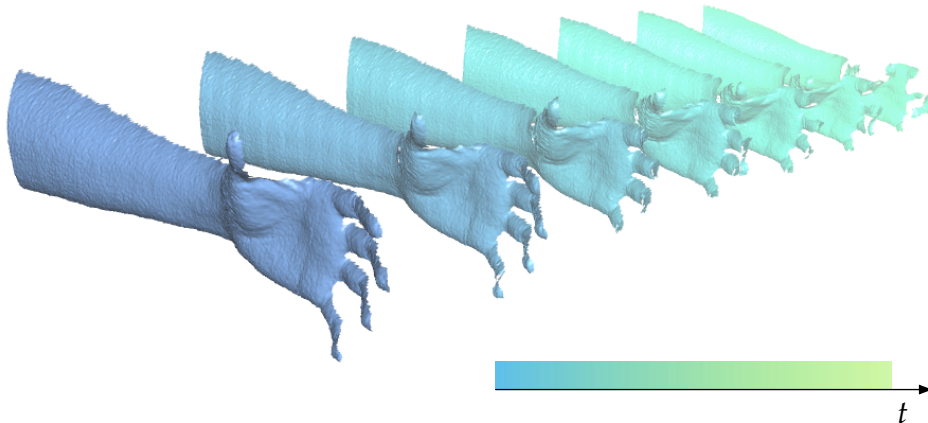


**Figure 1.1:** Input scan sequence of a grasping hand captured with a high speed 3-D scanner. The aim of this work is to build a complete 3-D model at a specific time instance from this sequence.

When acquiring moving and deforming objects (e.g. humans) using a fast 3-D scanner (c.f. [Weise et al. '07, Zhang et al. '06, Koninckx et al. '05, Rusinkiewicz et al. '02]), a dense sequence of varying shapes is produced as illustrated in Figure 1.1. Each scan does not cover the entire object and can represent a different region.

The aim of this work is to build a complete high-quality digital 3-D model of the object by performing *registration* on the whole scan sequence, which represents all exposed regions during the acquisition. Because the shapes are deformed, a particular point in time is chosen where all scans are aligned and un-deformed such that their corresponding regions coincide. We refer to this as *spatio-temporal*

registration. Ideally, the registered scans would look as if they were all taken simultaneously from different perspectives. A typical scenario for the reconstruction of a full human body would be that a person simply moves in front of the range scanner and a complete 3-D model is automatically generated.

The main challenge is to compute the right alignment and deformation for each scan based on the shared region between two scans. As the acquisition is time-coherent, the existence of such a common region can be assumed between two consecutive scans. Hence, a global correspondence over all partial shapes can be deduced by *transitivity*.

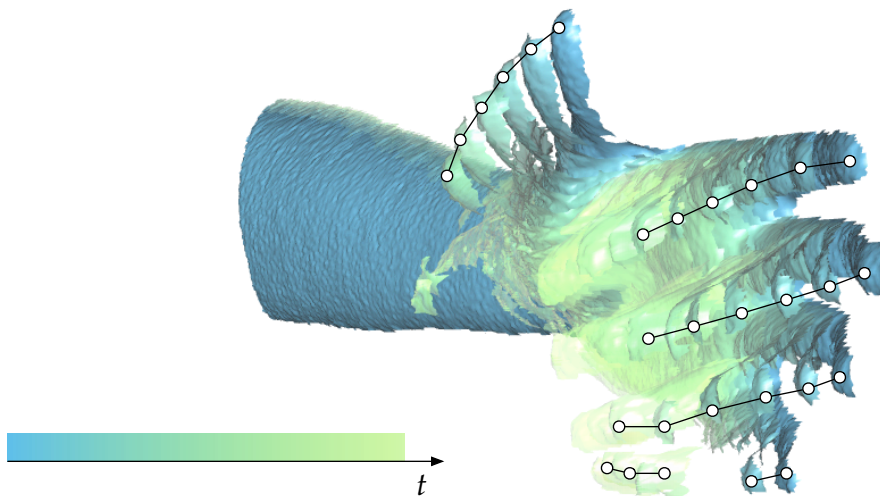


**Figure 1.2:** An accumulation of scans acquired over time  $t$  and shown within the same coordinate system. Corresponding points shown between individual scans show that spatio-temporal coherence is an important assumption to obtain a reliable estimation of correspondence. In particular, corresponding points might not be available in all frames.

However, correspondence between a pair of partial and deformed shapes is known to be a challenging problem. Nevertheless, similar to the *iterative closest point* (ICP) refinement [Besl & McKay '92, Chen & Medioni '92], the problem can be drastically simplified when correspondences are determined between two frames that are temporarily close (e.g. two consecutive scans). Figure 1.2 illustrates an example of corresponding points tracked on the finger tips of a scanned hand. Here, the deformation is small and the corresponding (or overlapping) regions can even be assumed to be large. Although pairwise registration of temporarily close scans seem to be feasible with relative ease, small registration errors would accumulate when global correspondences are related and large deformations of the object occur between a longer acquisition period. In addition to object deformations, 3-D acquisition data is typically affected by

noise, outliers, and acquisition holes due to occlusions and hardware limitations. This further complicates the task of correspondence.

This report has three purposes:

- First, we will discuss related work on scan registration and present a taxonomy to describe the specific spatio-temporal registration problem we are addressing (c.f. Section 1.1). This step will be helpful in formulating the necessary geometric assumptions about the input scans as will be discussed in Section 1.2.
- Next, a general approach for the registration of time coherent and deforming scans will be presented in Chapter 2. Here, we will propose a novel iterative framework for the registration of partial scans from all acquisition frames in order to obtain a complete 3-D model at a specific instance in time. In particular, the suggested method is built on top of known methods for the registration of rigid objects (c.f. Section 2.2) and uses well-established deformation algorithms for the pairwise matching of partial and deformed scans (c.f. Section 2.3).
- Eventually, we will demonstrate our algorithm on synthetic and real input data and synthesize the results in Section 3.1. One of our objectives is to explore the limits by using simplistic and general algorithms that make weak assumptions about the input data. Limitations of the proposed methods to specific sub-problems will be discussed in Section 3.2 and the implications for future research will be treated in Chapter 4.

## Contributions

The key innovation is that our registration problem envisions allowing large and complex object deformations without the use of any templates or manually selected correspondences, as these are difficult to obtain. To our knowledge, this is the first approach that explicitly addresses the problem of finding global correspondences fully automatically from a large set of deforming shapes that are densely sampled in space and time using a fast 3-D scanner. Hence, in contrast to previous work on non-rigid surface reconstruction techniques, we would design a realistic and practical scanning solution.

The proposed registration framework is an iterative approach that propagates scans from different frames into a particular time instance where the scans are deformed accordingly. Each deformation step is solved via a generalized ICP extended for non-rigid objects. Known techniques to individual sub-problems (e.g. correspondence, transformation, etc. . .) can be easily adapted for our purpose. Therefore, our method is a simple and general framework that is flexible

enough to integrate different algorithms that might use different assumptions about the input data.

The main objective of this report is not to describe a solution to the unsolved problem of registration of partial and non-rigid shapes. Instead, our framework will help to understand the main issues and identify the key assumptions necessary for further improvements. This work comes with a set of experiments where rather simplistic but well-established algorithms were adapted to their corresponding sub-problems. Promising preliminary results on real scan data have been discovered.

### Impact

As our ability to build high speed 3-D acquisition systems improves, so does the need to process the data they deliver. For instance, 3-D scanning devices are still mainly limited to special purpose applications such as full body scanners in the motion picture industry, building plaster casts to match a patient's anatomy in medicine, and quality control for the manufacturing of car components, to name a few.

However, during the last decade, a lot of attention have been paid within the graphics and vision community in pushing the limits of 3-D scanning technology, mainly in the context of cultural heritage (c.f. [Levoy et al. '00]), anthropology (c.f. [Allen et al. '03]), and other vision systems in robotics. Although numerous techniques successfully reproduce high quality 3-D models from objects in the physical world, they are often limited by high computation times and, most importantly, they are tedious and unintuitive to operate. These limitations are mainly due to the fact that many techniques only solve problems defined within a restrictive physical world setting. Also, the complexity of the algorithms is usually rather high.

However, a significant change is likely to occur in the near future as soon as real world geometry and dynamics can be reproduced fully automatically with a wide range of graphics applications. Here are two examples:

- For instance, the ability to reproduce a complete model for an arbitrary time would imply being able to reproduce one for all other acquisition frames as well. Consequently, this would provide a method for solving the problem of *surface reconstruction and motion capture on-the-go*, obviating motion capturing systems that require impractical and hard to calibrate markers.
- Moreover, the inter-frame correspondences would be fully determined and a consistent surface parametrization throughout all acquired frames could be defined. Being able to solve the global correspondence would be

a paramount step for *shape matching* applications such as *object recognition* or even *modeling* applications where *editing* could be done on entire scan sequences without knowing how the 3-D model was built.

## 1.1 Previous Work

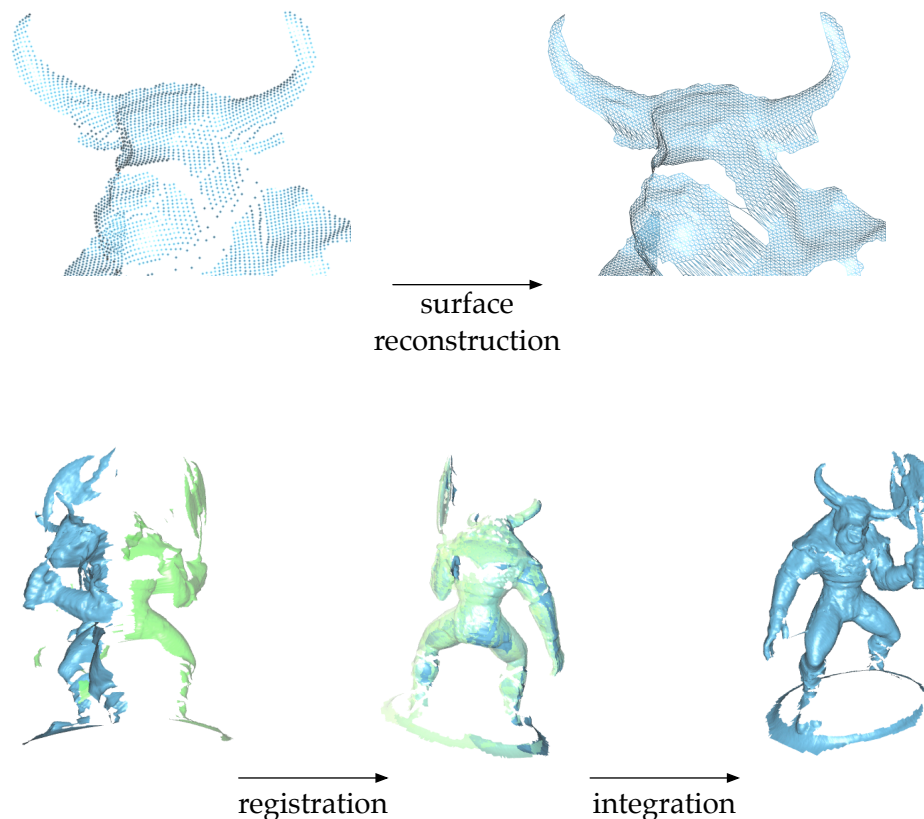


**Figure 1.3:** Main steps of a standard 3-D reconstruction pipeline demonstrated on a rigid object. The figurine has been scanned using the Minolta Vivid 900 laser scanner.

For optical 3-D acquisition systems that generate depth maps, registration methods play the central role in aligning the scans before obtaining a complete 3-D model via mesh integration. The standard 3-D reconstruction pipeline is illustrated in Figure 1.3. While a wide range of techniques has been investigated for the registration of rigid objects, less research has been conducted for deforming ones.

The registration stage is tightly coupled to the acquisition stage. In particular, depending on geometric and kinetic properties of the object being scanned and the depth maps being acquired, different approaches for registration will

be used. In other words, inverse problems with different assumptions about the input data will be tackled differently since different known and unknown variables are available.

To distinguish between different registration methods, we propose a taxonomy based on the assumptions made about the input data as shown in Table 1.1. The related work presented in this report is far from complete. However, we have included the most relevant and pioneering works on scan registration. We will now clarify the relationship between the assumptions made and the registration problems they imply.

input scans	rigid	deformable	
		small scale	large scale
sparse	[Gelfand et al. '05] [Huber & Hebert '01] [Pulli '99] [Roth '99] [Chen et al. '98] [Stoddart & Hilton '96] [Johnson & Hebert '97]	[Brown & Rusinkiewicz '07] [Brown & Rusinkiewicz '04]	[Mitra et al. '07b] [Anguelov et al. '05] [Anguelov et al. '04] [Allen et al. '03]
dense	[Rusinkiewicz et al. '02] [Rusinkiewicz & Levoy '01] [Chui & Rangarajan '00] [Chen & Medioni '92] [Besl & McKay '92]	[Mitra et al. '07a] [Amberg et al. '07] [Hähnel et al. '03]	this work

**Table 1.1:** A classification for registration methods

### Sparse or Dense Acquisitions

Sparse acquisition methods capture a few views of an object with overlapping regions while trying to cover the entire object as much as possible. The registration problem typically consists of finding correspondences based on local shape features from these overlapping regions and computing the transformations that align these scans. Most early works on 3-D reconstruction of static objects follow this registration procedure. Usually a refinement step is performed once a coarse alignment has been found.

On the other hand, dense acquisition methods use a high speed 3-D scanner to continuously sample an object from the real world. In particular, sampling is

dense in time and a huge amount of data is acquired. When the scanning frame rate is high enough for a moving object, consecutive frames become time coherent. The registration problem usually consists of using correspondences found in local neighborhoods and refining transformations subject to an optimization problem. In the rigid case, we also classify registration refinement algorithms such as ICP into the category of dense acquisitions since initial coarse alignments are assumed. We note that the direct aim of the refinement is not to build a complete 3-D model, but to find a more optimal alignment.

Nevertheless, in our setting, we make use of the time-coherent data to track correspondences similar to the approach presented in [Rusinkiewicz et al. '02] with the only difference that we allow large deformations over a certain acquisition period.

### **Rigid or Deformable Objects**

For rigid objects, the transformations computed by the registration method stay within the group of Euclidean transformations. Since only 6 parameters have to be determined (3 for rotation and 3 for translation), the focus is often on extracting and matching a large number of local shape features in order to solve for an optimal solution of an over-determined system.

On the other hand, registration becomes much more challenging when we allow the scanned object to undergo deformations. Without any prior knowledge, a general deformation would have an infinite number of degrees of freedom. More restrictive assumptions about the deformation behavior are therefore necessary in order to formulate an appropriate deformation model. However, finding the right deformations requires knowledge about corresponding regions. Here, the correspondence problem becomes a difficult task since matching has to be performed between different shapes. For sparse acquisitions, for instance, the focus is usually on extracting near rigid regions, as in the case of articulated objects (c.f. [Mitra et al. '07b]), or on finding globally optimal inter-shape correspondences using a complete template model (c.f. [Anguelov et al. '05, Anguelov et al. '04]).

For dense acquisitions, as in our case, the deformations between consecutive frames are small and we can make use of this inter-frame coherence to deduce consistent correspondences.

### **Small or Large Object Deformations**

For deformable objects, we further distinguish between our definition of small- and large-scale deformations.

We refer to registrations of objects with small scale deformation as those where deformation of the scanned object is not explicitly intended. And if

so, it is limited to some extent. For instance, in [Brown & Rusinkiewicz '07, Brown & Rusinkiewicz '04], acquired scans of rigid objects are assumed not perfectly rigid because of scanning hardware limitations such as calibration errors. Giving more degrees of freedom in the transformation allows better preservation of high frequency details. Similarly, when deformations of acquired objects are limited, recent methods based on dense acquisitions have successfully registered partial and deformable scans, using estimations of motion as in [Mitra et al. '07a] or by extending ICP for non-rigid shapes (c.f. [Amberg et al. '07, Hähnel et al. '03]).

We define the registration problem of objects with large-scale deformations as the case where no restrictions are imposed on the amount of deformations undergone during the whole acquisition process. Note that, while assumptions are made on the deformation model, we do not limit the distance traversed within the corresponding *deformation space*. In [Mitra et al. '07b], for example, correspondence is computed by extracting rigidness of shapes using the symmetry detection algorithm from [Mitra et al. '06]. In this way, corresponding regions are matched and deformed for the registration of partial scans. However a complete template model which undergoes the deformation is required as is the case with the approaches presented in [Angelov et al. '05, Angelov et al. '04, Allen et al. '03].

To the best of our knowledge, there is no work so far that explicitly addresses the registration problem by allowing large scale deformations without the use of any templates. We therefore suggest an approach that uses dense scan acquisitions for solving the correspondence problem. With this design, we have successfully performed the registration of objects with small-scale deformations. Promising future directions from Section 4.2 provide potential solutions for larger scale deformations.

## 1.2 Assumptions Analysis

Making assumptions about the shape of input scans is equivalent to restricting the scope for real world acquisitions. On the other hand, it is required to simplify the registration problem and the art is to find the right trade-off.

We impose restrictions on geometric and kinetic properties of the real world object and the input shapes after the acquisition. The registration algorithm must be able to handle the underlying assumptions, which obviously are tightly coupled to the acquisition technique. Therefore, we restrict ourselves to scans that are produced by 3-D scanners equivalent to those based on *structured lights* (c.f. [Weise et al. '07, Zhang et al. '06, Li et al. '06, Koninckx et al. '05,

Zhang et al. '02, Rusinkiewicz et al. '02]). Similar properties can be found in other high speed 3-D scanning technologies.

### **Assumptions About the Scanned Object**

The scanned object is assumed be bounded by an oriented smooth manifold surface. Consequently, local surface parametrizations exist and differentiations are possible for extracting higher order shape information such as normals and local curvatures.

Moreover, we allow the surface to undergo global rigid motions provided the transformation is smooth. For instance, the motion at close time instances must be similar. In order to perform registration of deformable objects, we permit non-rigid components in the transformations. We also require these deformations to behave smoothly. In addition to temporal deformation smoothness, we make the assumption that the deformation of spatially close points on a surface are similar as well.

Although not covered by our preliminary work, assumptions about isometry of the deformation model and as-rigid-as-possible deformations for articulated objects would be important considerations for future research in order to further improve registration robustness.

### **Restrictions Imposed by Acquisition Device**

Since our registration method is performed directly on the acquired scans, hardware limitations must be considered when making assumptions about the input data. For instance, the spatial sampling density (depth map resolution) can be assumed to be high but it is still limited. Thus, high frequency details can be captured as long as they satisfy the Nyquist limit (c.f. [Li '05] for more details). Similarly, the same restriction applies to the temporal sampling density, which is determined by the acquisition frame rate. In order to cope with the assumption of smooth motion in the scanned object, the scanning speed must be sufficiently high.

Other than sampling limitations, input scans typically suffer from high frequency noise and outliers mostly due to measurement inaccuracies, non-cooperative surface properties, and optical triangulation errors depending on the range imaging technology (c.f. Figure 1.4). Both sources of errors can usually be treated effectively with well-established mesh or point processing methods (c.f. [Li '05, Weyrich et al. '04]).

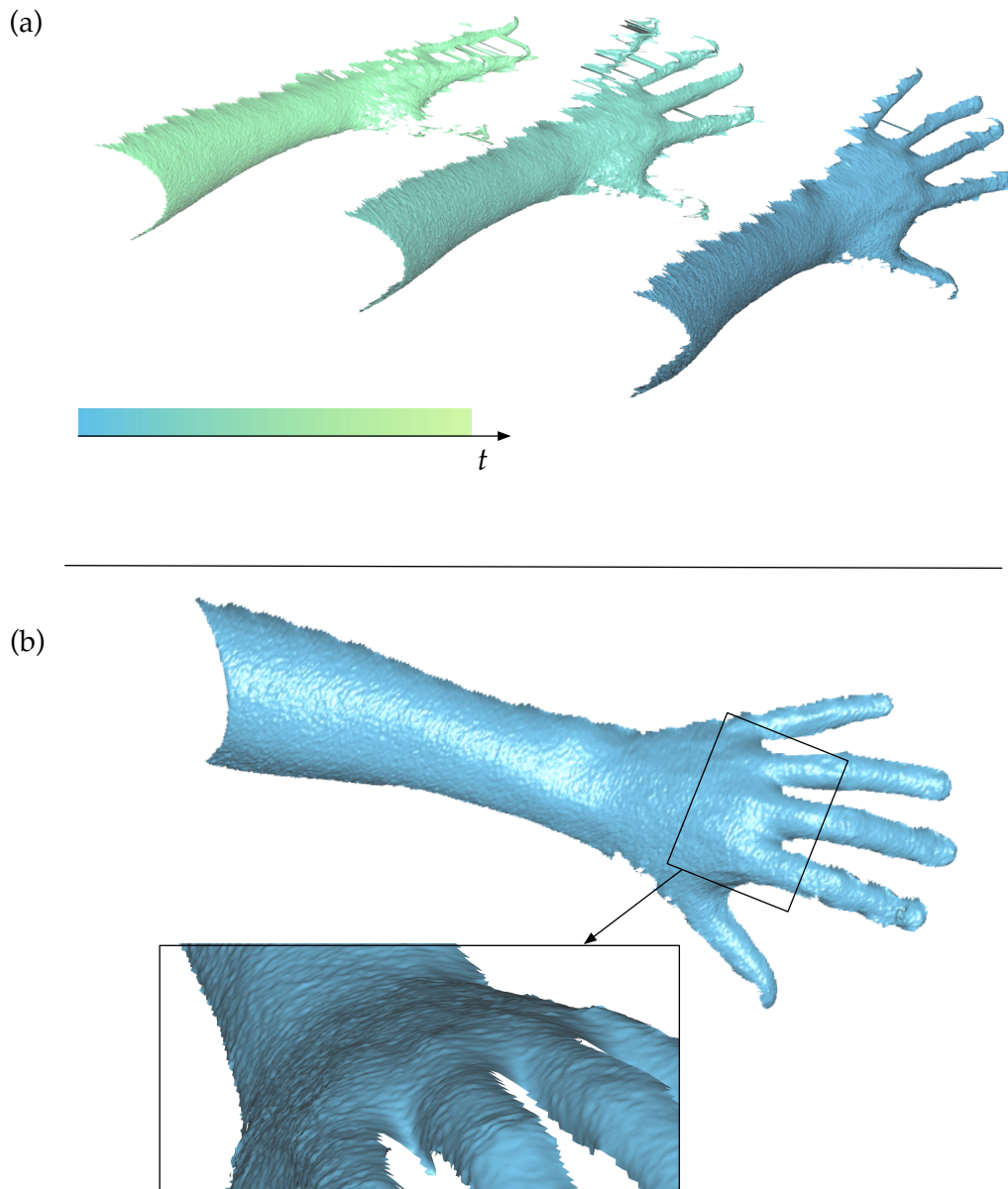


**Figure 1.4:** (a) Raw scan data affected by noise and outliers. Triangle with long edges between fingers are due to triangulation in image space during surface reconstruction. Artifacts around the boundaries of the scans are due to limitations of the acquisition method when object motion is too fast (this issue only exists for certain 3-D scanning technologies). (b) The high resolution scan exhibits a considerable amount of high frequency noise as shown in the enlarged figure.

# Chapter 2

## Spatio-temporal Registration

This chapter introduces the methodology of our proposed spatio-temporal registration approach. The proposed framework finds a deformation for the scans of each frame in order to compute their shapes at a specific time instance. For this, a general registration scheme is proposed in Section 2.1 that propagates pairwise correspondences and deformations from all frames toward the target time instance. Each propagation step is solved using an ICP-based registration refinement process. A more detailed description of the pairwise correspondence and transformation stage is given in Section 2.2 and 2.3, respectively. Although correspondence and deformation could have been formulated as the optimal solution of a single global minimization problem, we choose to decouple both stages. This way, the problem becomes significantly simpler and known techniques can be used for analysing and solving individual sub-problems.

### 2.1 A General Framework

Inspired by global registration algorithms based on ICP for rigid objects, we present a simple registration scheme for obtaining a complete 3-D model from a sequence  $\mathcal{S} = (\mathcal{M}_1, \dots, \mathcal{M}_n)$  of  $n$  partial and deforming surfaces  $\mathcal{M}_i \subset \mathbb{R}^3$  acquired at time  $t_i$ . The acquisition is uniformly time sampled so that we can write  $t_i = i \in \mathbb{N}$ .

#### Registration for a Single Time Instance

For non-rigid registrations between a pair of scans, the source scan  $\mathcal{M}_i$  is deformed onto the target scan  $\mathcal{M}_j$  which remains unchanged. The deformed scan of  $\mathcal{M}_i$  is denoted  $\mathcal{M}_i^{(j)} = \varphi_i(\mathcal{M}_i, \mathcal{M}_j)$  with deformation  $\varphi_i$  (c.f. Section 2.3) and

semantically belongs to the target time  $j$ . Here,  $\varphi(\mathcal{M}_i, \mathcal{M}_j)$  is a hypothetical optimal transformation deduced from the pair  $\mathcal{M}_i$  and  $\mathcal{M}_j$ . We note that

$$\mathcal{M}_i^{(i)} = \mathcal{M}_i \quad \text{and} \quad \mathcal{M}_i^{(k)} = \mathcal{M}_i^{(j)} \quad \forall k > j \quad .$$

In particular, the registration computes an optimal  $\mathcal{M}_i^{(j)}$  such that the corresponding regions  $\mathcal{N}_i \subset \mathcal{M}_i$  and  $\mathcal{N}_j \subset \mathcal{M}_j$  are perfectly aligned for time  $j$ , i.e.  $\mathcal{N}_i^{(j)} = \mathcal{N}_j$  with  $\mathcal{N}_i^{(j)}$  an *optimally* deformed surface of  $\mathcal{N}_i$ .

In order to obtain the complete 3-D model  $\mathcal{M}_{\text{tot}}$  at a specific time instance, the scans of all frames  $i \neq j$  must be deformed to the instance in time of a particular target scan  $j$ . Without loss of generality, we choose this time instance to be the last frame  $n$  of the acquisition. Our objective is then to find the deformations  $\varphi$  for all scans  $\mathcal{M}_i$  to eventually obtain

$$\mathcal{M}_{\text{tot}} = \bigcup_i \mathcal{M}_i^{(n)} \subset \mathbb{R}^3 \quad .$$

However, pairwise registration is only possible when all scans have sufficiently large corresponding regions with this last frame. In general, this situation is unlikely to occur as our partial input scans are trying to cover the entire object from different views. Consequently, we use from Section 1.2 the assumption that scans that are close in time have large corresponding regions. Therefore, we first restrict ourselves to pairwise registrations between consecutive scans  $\mathcal{M}_i$  and  $\mathcal{M}_{i+1}$ . Thus, the optimal deformation between consecutive scans can be denoted  $\varphi_i = \varphi(\mathcal{M}_i, \mathcal{M}_{i+1})$ .

By applying the  $\varphi_i$  for  $i = 1 \dots n - 1$ , all scans are incremented in time:

$$\varphi_i : \mathcal{M}_i \mapsto \mathcal{M}_i^{(i+1)}$$

where  $\mathcal{M}_n$  remains unchanged. In particular  $\mathcal{M}_i^{(i+1)}$  belongs to time  $i + 1$ .

More generally, the deformation of a deformed scan  $\mathcal{M}_i^{(j)}$  is given by:

$$\varphi_i : \mathcal{M}_i^{(j)} \mapsto \mathcal{M}_i^{(j+1)} \quad \text{with} \quad i \leq j \leq n - 1 \quad . \quad (2.1)$$

This yields the following registration scheme when the deformations in Equation 2.1 are repeated  $n - 1$  times:

$$\begin{array}{ccccccc}
\mathcal{M}_1 & \mapsto & \mathcal{M}_1^{(2)} & \mapsto & \dots & \mapsto & \mathcal{M}_1^{(n-1)} & \mapsto & \mathcal{M}_1^{(n)} \\
\mathcal{M}_2 & \mapsto & \mathcal{M}_2^{(3)} & \mapsto & \dots & \mapsto & \mathcal{M}_2^{(n)} & & \\
\vdots & & \vdots & & \vdots & & & & \\
\mathcal{M}_{n-2} & \mapsto & \mathcal{M}_{n-2}^{(n-1)} & \mapsto & \mathcal{M}_{n-2}^{(n)} & & & & \\
\mathcal{M}_{n-1} & \mapsto & \mathcal{M}_{n-1}^{(n)} & & & & & & \\
\mathcal{M}_n^{(n)} = \mathcal{M}_n & & & & & & & & 
\end{array}$$

$$\begin{array}{c}
\underbrace{\hspace{10em}}_{\varphi_i} \quad \underbrace{\hspace{10em}}_{\varphi_i} \quad \dots \quad \underbrace{\hspace{10em}}_{\varphi_i} \\
\underbrace{\hspace{10em}}_{\varphi_i^2} \\
\underbrace{\hspace{10em}}_{\varphi_i^{n-1}}
\end{array}$$

which can be summarized by computing

$$\varphi_i^{n-i} : \mathcal{M}_i \mapsto \mathcal{M}_i^{(n)} \quad (2.2)$$

for  $i = 1 \dots n - 1$ . A step by step visualization for each iteration  $i$  is shown in Figure 2.1.

Ultimately, the deformed scans  $\mathcal{M}_i^{(n)}$  would only exist for the last point in time  $n$  (labeled in blue) and the full global correspondence would be determined via transitivity from these aligned scans. Hence, the proposed registration framework for computing  $\mathcal{M}_{\text{tot}}$  is simply  $n - i$  iterations of pairwise registrations between all consecutive scans  $\mathcal{M}_i$  and  $\mathcal{M}_{i+1}$ . In total,  $\frac{n(n-1)}{2}$  pairwise registrations (i.e. deformations) are required.

### Pairwise Registration of Integrated Scans

As mentioned earlier, a pairwise registration between consecutive scans  $\mathcal{M}_i^{(j)}$  and  $\mathcal{M}_{i+1}^{(j)}$  is, in general, insufficient for computing an optimal deformation  $\varphi_i(\mathcal{M}_i^{(j)}) = \mathcal{M}_i^{(j+1)}$ , as illustrated on an example in Figure 2.2.

Fortunately, when the registration scheme from Equation 2.2 is applied for  $i = 1 \dots n - 1$ , the number of available scans at instance  $j$  increases with  $i$ , as shown in the following equation:

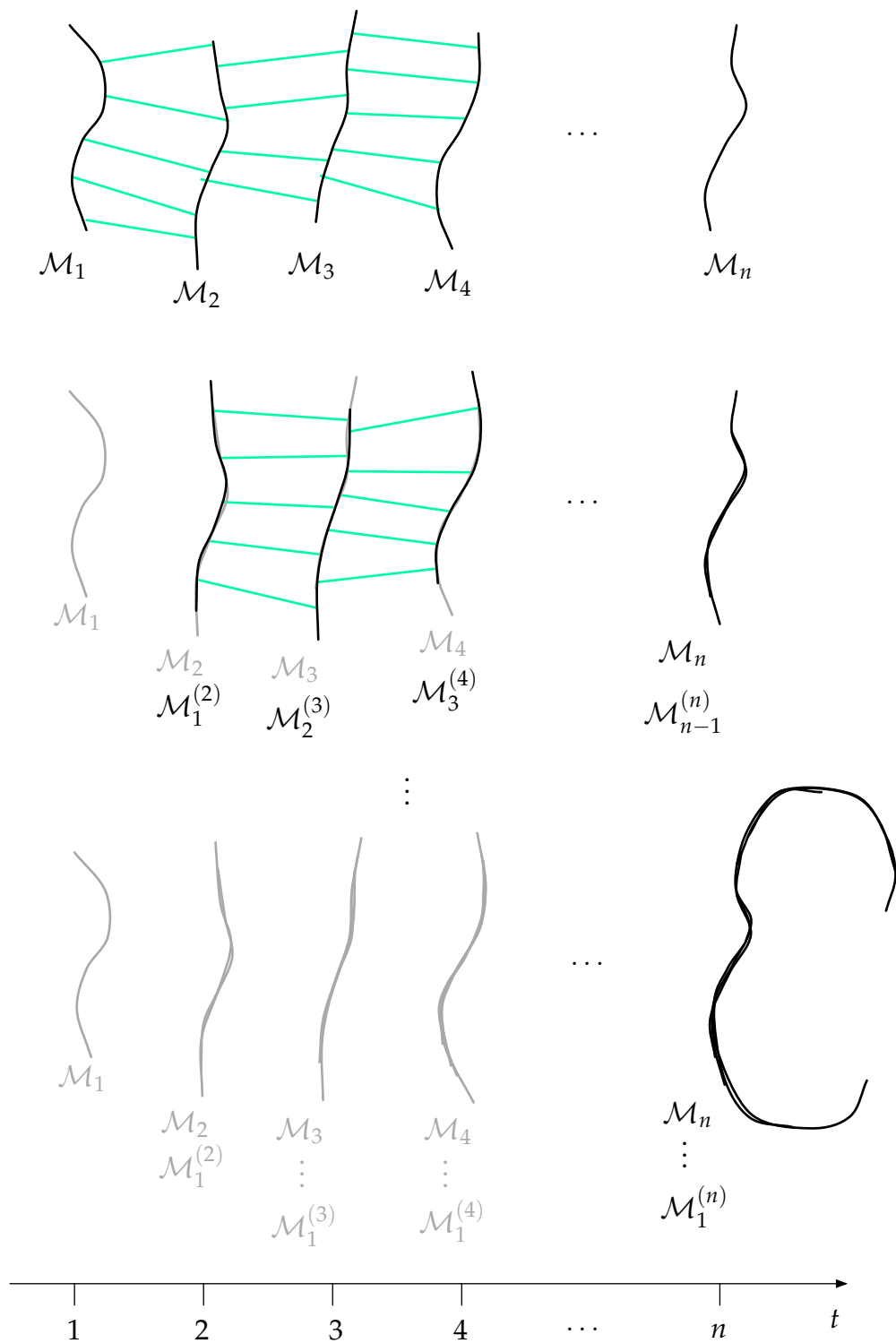


**Figure 2.1:** An idealized step by step illustration for each iteration of the registration scheme in 2-D.

$$\begin{array}{ccccccc}
\mathcal{M}_1^{(1)} & \mapsto & \mathcal{M}_1^{(2)} & \mapsto & \dots & \mapsto & \mathcal{M}_1^{(n-1)} & \mapsto & \mathcal{M}_1^{(n)} \\
& & \mathcal{M}_2^{(2)} & \mapsto & \dots & \mapsto & \mathcal{M}_2^{(n-1)} & \mapsto & \mathcal{M}_2^{(n)} \\
& & & & \ddots & & \vdots & & \vdots \\
& & & & & & \mathcal{M}_{n-1}^{(n-1)} & \mapsto & \mathcal{M}_{n-1}^{(n)} \\
& & & & & & & & \mathcal{M}_n^{(n)} .
\end{array}$$

In particular, the deformation  $\varphi_i(\mathcal{M}_i^{(j)}) = \varphi(\mathcal{M}_i^{(j)}, \mathcal{M}_{i+1}^{(j+1)}) = \mathcal{M}_i^{(j+1)}$  can be deduced not only from a pair of source and target scans,  $\mathcal{M}_i^{(j)}$  and  $\mathcal{M}_{i+1}^{(j+1)}$ , but also from all  $\mathcal{M}_k^{(j+1)}$  with  $j+1 < k \leq n-1$ .

We therefore call the union of all valid target scans:

$$\mathcal{M}_{\text{tot}}^{(j+1)} = \bigcup_{k=j+1}^{n-1} \mathcal{M}_k^{(j+1)} \quad (2.3)$$

the *integrated target scan* of a source  $\mathcal{M}_i^{(j)}$ . We note that the union only makes sense for perfectly aligned corresponding regions and thus, the existence of the optimal deformations. We then define a deformation between a source scan and its corresponding integrated target scan to be  $\hat{\varphi}_i = \varphi(\mathcal{M}_i^{(j)}, \mathcal{M}_{\text{tot}}^{(j+1)})$ .

Hence, our presented registration scheme of Equation 2.2 is extended to:

$$\hat{\varphi}_i^{n-i} : \mathcal{M}_i \mapsto \mathcal{M}_i^{(n)} \quad \text{for } i = 1 \dots n-1. \quad (2.4)$$

Since more data is used for correspondence at a certain frame, this algorithm would be generally more robust than the one presented in Equation 2.2. However, the computational cost is obviously higher. A more efficient way to handle cross-scan correspondences remains an interesting topic for future research.

### Refinement of the Pairwise Registration

So far, the hypothesis was that an optimal deformation  $\hat{\varphi}_i$  is deduced from a source-target pair,  $\mathcal{M}_i^{(j)}$  and  $\mathcal{M}_{\text{tot}}^{(j+1)}$ , as long as the corresponding region between both scans is sufficiently large. However, only a sub-optimal estimation is possible, as it is the case with all non-global registration methods where the introduction of registration errors have to be taken into account. From now on, we refer to our source and target surfaces as  $\mathcal{M}_s = \mathcal{M}_i^{(j)} \subset \mathbb{R}^3$  and  $\mathcal{M}_t = \mathcal{M}_{\text{tot}}^{(j+1)} \subset \mathbb{R}^3$  since only pairwise registrations are considered.

The goal is to determine a deformation of  $\mathcal{M}_s$  that aligns the corresponding regions of the scan pairs by satisfying the geometric and kinetic properties of the

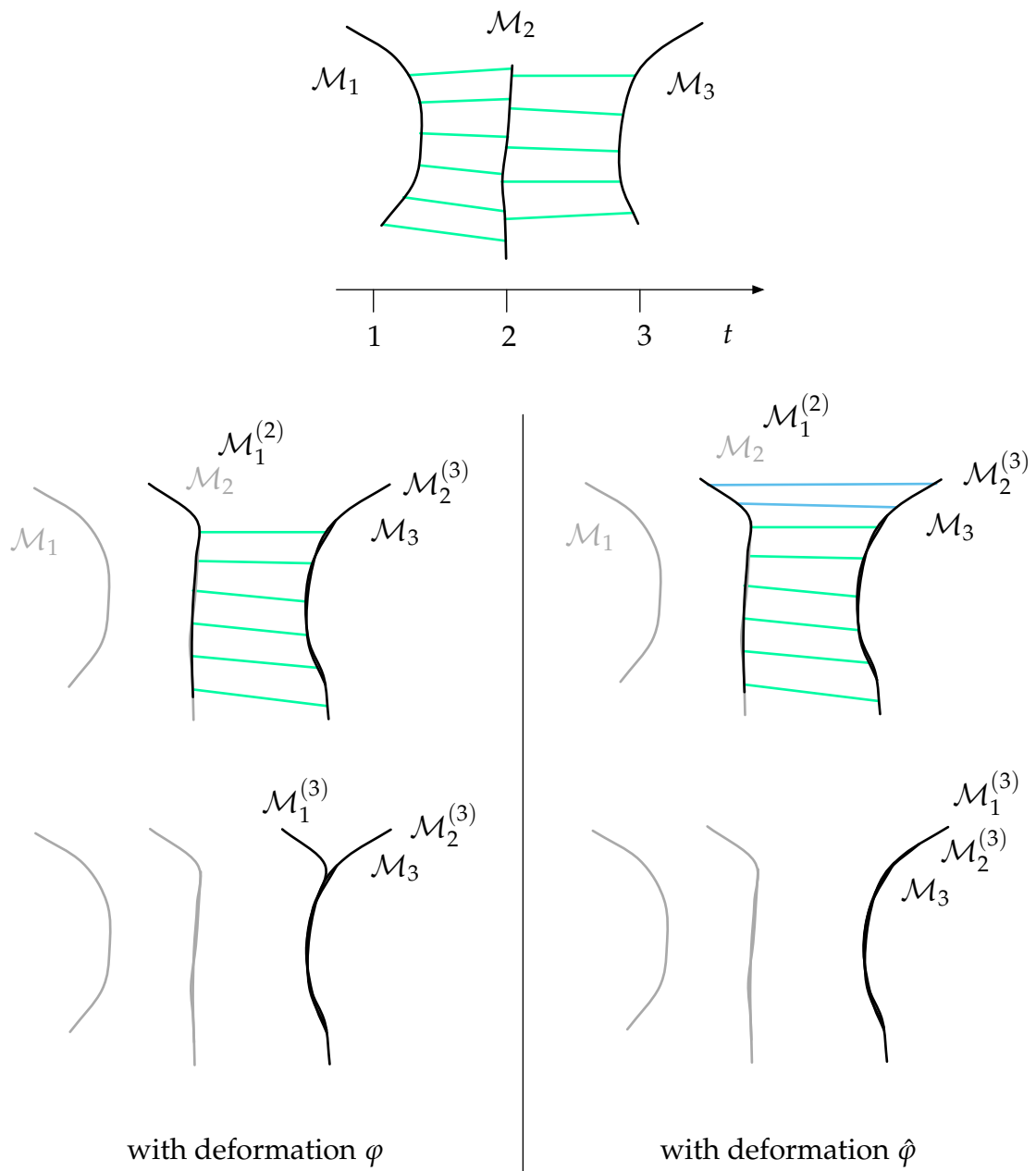


**Figure 2.2:** This example shows a case where a registration with integrated scans is necessary (right column).

scanned object as presented in Section 1.2. While the restrictions imposed by the scanned object can be implicitly encoded in the deformation model (c.f. Section 2.3), the *displacement* constraints that dictate the deformation itself depend on the point-to-point correspondences of the corresponding regions  $\mathcal{N}_S \subset \mathcal{M}_S$  and  $\mathcal{N}_t \subset \mathcal{M}_t$ . Hence our registration problem can be broken down into *correspondence* and *transformation* sub-problems.

The observation here is that we have an almost identical setting as with traditional ICP refinement problems. The difference is that we are interested in the registration of a vast collection of scans with considerably large and complex deformations occurring over a certain acquisition period. However, since the number of pairwise registrations is quadratic with the number of input scans, the accumulation of deformation errors would be one of the core issues, which is especially the case for large deformations. Moreover, the transformation must be general enough to cope with complex deformations such as articulated and non-rigid objects. Being general, the deformation model is also more likely to introduce errors.

With these considerations in mind, we suggest following the design of the well-known pairwise ICP algorithm as illustrated in Figure 2.3 and adapting each step to our purpose. The sampling, correspondence, and pruning stages will be discussed in detail in Section 2.2. They are followed by the deformation procedure which is then presented in Section 2.3.

The justification for using an iterated process is that the estimation of an optimal deformation and its correspondence form a mutual dependency. For instance, good correspondences are easier to estimate when the scans are close in shape and position (i.e. small deformation). On the other hand, a correct deformation highly depends on the quality of the correspondences.

Unlike ICP methods for rigid objects, the formulation of a termination criterion is ill-posed. In fact, the ideal condition to abort the loop is when corresponding regions are perfectly aligned. However, this situation cannot be explicitly determined since no temporal consistent parametrization is available. Therefore, we specify the number of iterations for the loop similar to other works on deformations for shape matching (c.f. [Sumner & Popović '04, Allen et al. '03]).

## 2.2 Pairwise Correspondence

Given a source  $\mathcal{M}_s$  and a target  $\mathcal{M}_t$ , we now look at how to find point-to-point correspondences for determining the deformation displacements. Since the motion of the scanned object is assumed to be smooth and the acquisition frame rate is high, two corresponding points must be close. Moreover, we assume the deformation between two acquired scans to be small. Accordingly, their shapes have to be similar.

Consequently, a reliable and efficient way to estimate corresponding points on  $\mathcal{M}_t$  is to search in the vicinity of points sampled from  $\mathcal{M}_s$ . Relying solely on point positions, computing the Euclidean *closest point* would seem to be most appropriate. However, in the context of rigid ICP, it is well understood that, under certain conditions, other estimations can yield faster refinement conver-

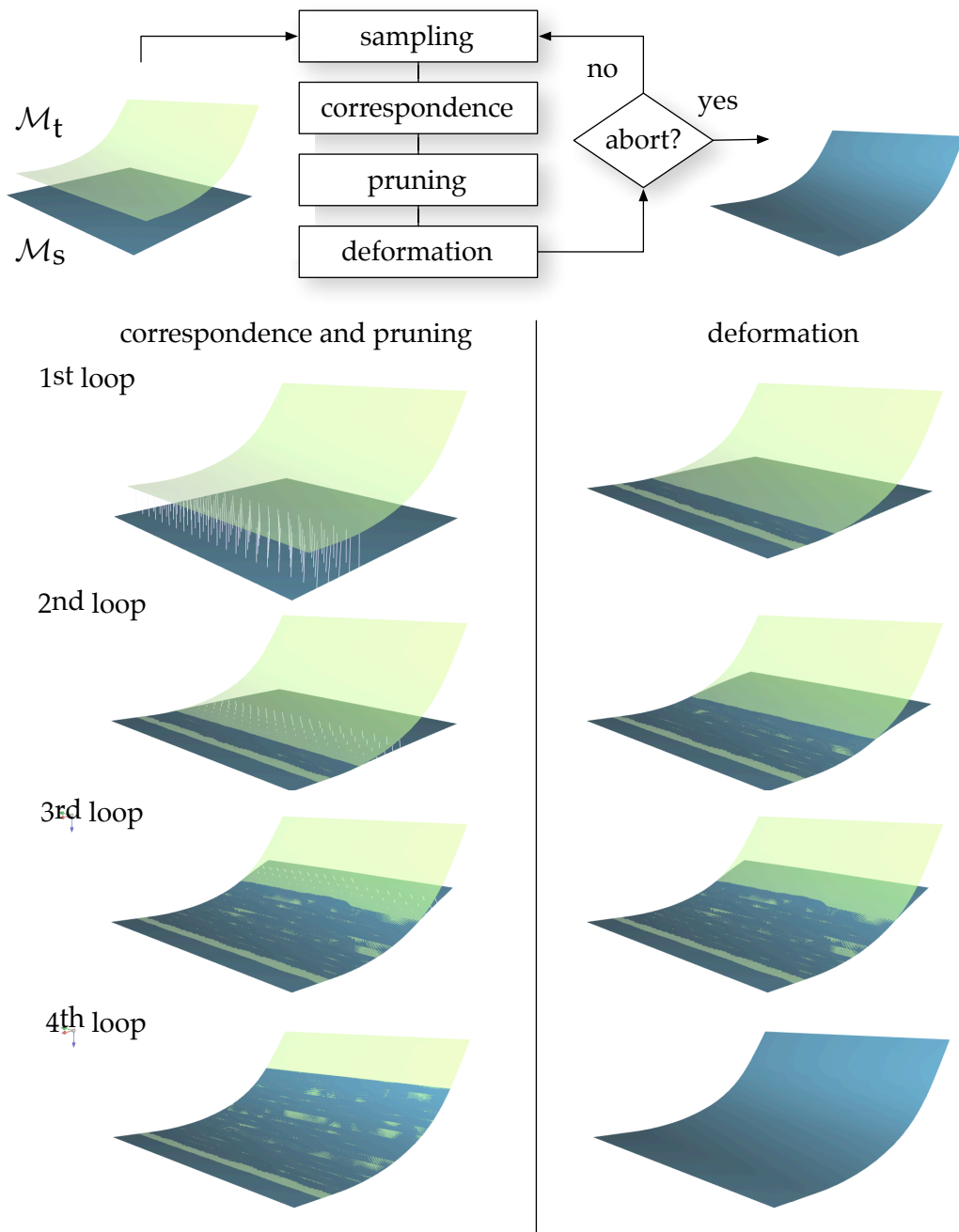


**Figure 2.3:** The data flow of the ICP algorithm for non-rigid objects is shown above. Each refinement step between a plane (blue) and its deformed shape (green) is shown below where the point-to-point correspondences are shown in white.

gence such as the projection to the tangent plane. As the effect of both approaches on the convergence on non-rigid ICP is unclear, we will examine both

avenues more closely. Note that both methods do not rely explicitly on any specific geometric features of the surface. They depend on the curvature of  $\mathcal{M}_S$  and  $\mathcal{M}_t$ , but do not use it for correspondence.

### Sampling

Before any correspondence is determined, many approaches suggest a particular sampling strategy for faster convergence and more efficient processing. An extensive survey is presented in [Rusinkiewicz & Levoy '01], in which an interesting method is introduced: namely, a sampling technique that maximizes the distribution of normals among selected points. This technique has been demonstrated to be particularly effective for smooth shapes with sparse features. While better results are likely to be achieved with the aid of more advanced sampling techniques, we choose to use all available mesh vertices  $\mathbf{x}_i \in \mathcal{M}_S$  with  $i = 1, \dots, n$  as in [Besl & McKay '92] for the sake of simplicity as our input scans are already dense and uniformly sampled. However, if efficiency is desired, we perform a simple *isotropic remeshing* as described in [Botsch & Kobbelt '04] to reduce the number of points while keeping the point density as uniform as possible.

### Closest Surface Point

We define the closest point of a point  $\mathbf{x}_i \in \mathcal{M}_S$  on a triangle mesh  $\mathcal{M}_t$  to be

$$\mathbf{c}_i = \pi_{\text{closest}}(\mathbf{x}_i) = \underset{\mathbf{c}_i}{\operatorname{argmin}} \|\mathbf{c}_i - \mathbf{x}_i\|^2 \quad \text{with } \mathbf{x}_i \in \mathcal{M}_S \quad \text{and} \quad \mathbf{c}_i \in \mathcal{M}_t \quad .$$

The closest surface point is a good estimate for the correspondence when  $\mathcal{M}_S$  and  $\mathcal{M}_t$  are close and have almost the same shape. Our assumptions presented in Section 1.2 satisfy this condition. Moreover,  $\mathbf{c}_i$  can be computed efficiently in  $O(\log n)$  using a spatial search data structure such as a *kd tree* (c.f. [Bentley '75]) with triangles as geometric entities. In particular,  $\mathbf{c}_i$  is the closest point on the closest triangle to  $\mathbf{x}_i$  retrieved with the *kd tree*.

Many convergence properties from rigid ICP using the closest point as correspondence (c.f. [Gelfand et al. '03]) are similar to those of our registration framework with deformable scans. For instance, because of the local nature of the minimization, the convergence can be slow, especially in the case of tangential motions along the surface. The evidence of the linear convergence of rigid ICP using closest point can be found in [Pottmann et al. '06].

### Tangent Plane Projection

A different strategy for finding corresponding points of  $\mathbf{x}_i \in \mathcal{M}_S$  consists of performing an orthogonal projection on the tangent plane of a point  $\mathbf{r}_t \in \mathcal{M}_T$ .  $\mathbf{r}_t$  is the intersection of the ray originating from  $\mathbf{x}_i$  in the direction of its normal. We refer the corresponding points of  $\mathbf{x}_i$  to as:

$$\mathbf{c}_i = \pi_{\text{tangent}}(\mathbf{x}_i)$$

and compute it as follows. The ray originating from  $\mathbf{x}_i$  is given by the explicit representation  $\mathbf{r}(\alpha) = \alpha \mathbf{n}_i^{(S)} + \mathbf{x}_i$  with normal vector  $\mathbf{n}_i^{(S)}$ . Intersecting  $\mathbf{r}(\alpha)$  with the triangle mesh  $\mathcal{M}_T$  yields the *normal foot point*  $\mathbf{r}_t = \mathbf{r}(\alpha_t) \in \mathcal{M}_T$  with normal  $\mathbf{n}_i^{(T)}$ . For  $\|\mathbf{n}_i^{(T)}\| = 1$  we obtain the *tangent plane projection*:

$$\mathbf{c}_i = (I - \mathbf{n}_i^{(T)} (\mathbf{n}_i^{(T)})^T)(\mathbf{x}_i - \mathbf{r}_t) + \mathbf{r}_t \quad .$$

This method has first been proposed for a rigid iterative closest point method in [Chen & Medioni '92] and the main idea is to let flat and spherical regions slide along each other (c.f. [Gelfand et al. '03]). Indeed, when the initial source and target surfaces are very close, convergence has been proven to be faster than the closest point method as observed in [Pottmann et al. '04, Pottmann & Hofer '03]. Note that for the analysis of rigid ICP convergence, this point-to-plane method can even achieve local quadratic convergence for a zero residual problem if additional regularization and step size control is performed.

In our case, this convergence analysis is more difficult to perform since our optimal solution is found when the corresponding regions of a deformed  $\mathcal{M}_S$  and  $\mathcal{M}_T$  perfectly match. Unfortunately, the problem of defining correspondence is ill-posed.

However, the projection to tangent plane method can be computed efficiently as well by using a spatial data structure (e.g. a kd tree) for searching the intersections  $\mathbf{r}_t$  similarly to ray-tracing acceleration techniques.

Considering input scans being affected by high frequency noise, it is better to compute stable normals  $\mathbf{n}_i^{(S)}$  and  $\mathbf{n}_i^{(T)}$  by estimating normals from local neighborhoods with larger radii. An extensive analysis on the estimation of surface normals in noisy scan data can be found in [Mitra & Nguyen '03].

### Correspondence Pruning

A simple heuristic presented in [Pauly et al. '05] suggests performing a bi-directional closest point search and to prune the correspondences which have a high deviation from their original vertices. More precisely, let

$$\mathbf{b}_i = \pi_{\text{closest}}^2(\mathbf{x}_i) \in \mathcal{M}_S$$

be the closest point of  $\mathbf{c}_i = \pi_{\text{closest}}(\mathbf{x})_i$  on the mesh  $\mathcal{M}_S$ . When  $\delta_i = \|\mathbf{b}_i - (\mathbf{x})_i\|$  is larger than a certain threshold  $\sigma$ , we decide to discard the correspondence for  $\mathbf{c}_i$ . A reasonable estimate for  $\sigma$  is to take the average local sample spacing of vertices in  $\mathcal{M}_S$  as illustrated in Figure 2.4.

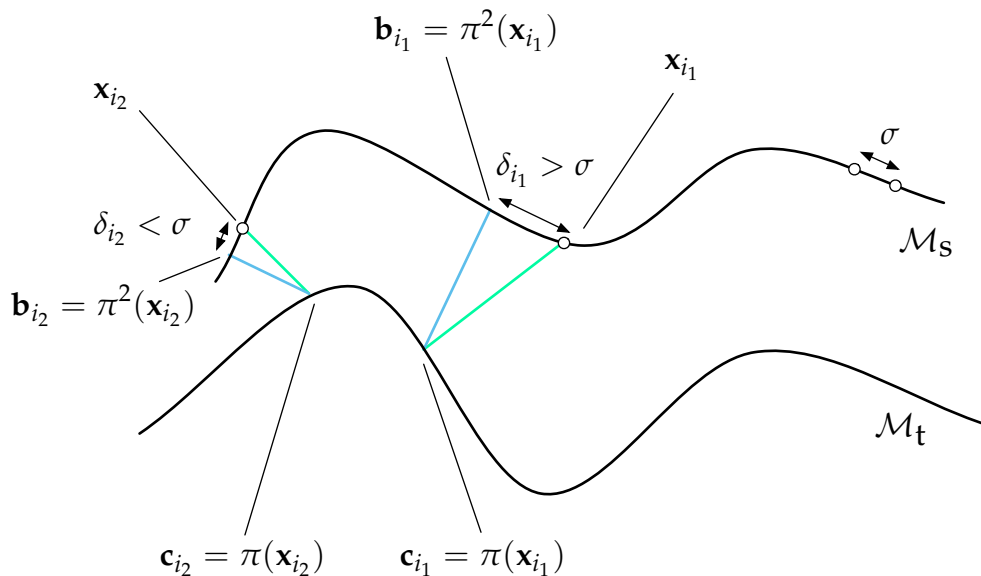


**Figure 2.4:** In this example,  $\mathbf{x}_{i_1}$  will be pruned because its bidirectional closest point  $\mathbf{b}_{i_1}$  has a deviation  $\delta_{i_1} > \sigma$  whereas  $\mathbf{x}_{i_2}$  and  $\mathbf{c}_{i_2}$  form a valid correspondence since  $\delta_{i_2} < \sigma$ .

## 2.3 Deformation Model

The formulation of a deformation model determines the degrees of freedom of the transformation undergone during the iterated registration process described in Section 2.1. If an overly general deformation model is chosen, it is likely that an arbitrary shape would result from the registration. When it is too restrictive (e.g. a near rigid motion), incorrect correspondences would be computed and the scans would converge to an undesired local minima.

While an extensive survey on different deformation techniques is presented recently in [Botsch & Sorkine '07], we choose to adapt the deformation algorithm developed in [Sumner & Popović '04] within the context of correspondence computation for deformation transfer. The method is general enough to represent arbitrary non-linear deformations since it has proven its ability to derive complete deformations from complex triangle mesh animations. Moreover, it preserves deformation smoothness which suits the requirements of our assumptions made about the scanned object as presented in Section 1.2.

The general deformation model is represented by a set of affine mappings

$$\tilde{\mathbf{x}} = \Phi_l(\mathbf{x}) = A_l \mathbf{x} + \mathbf{a}_l \in \mathbb{R}^3 \quad \text{with} \quad l = 1 \dots m$$

for each triangle  $\mathcal{T}_l$  of a triangle mesh  $\mathcal{M} \subset \mathbb{R}^3$  with  $m$  triangles.  $\Phi_l$  relates the deformed vertex  $\tilde{\mathbf{x}}$  to the undeformed  $\mathbf{x} \in \mathcal{T}_l$ . In particular, the underlying linear map  $A_l \in \mathbb{R}^{3 \times 3}$  encodes the change in scale, orientation, and skew induced by the deformation of the triangle with vertices

$$\mathbf{x}_p, \mathbf{x}_q, \mathbf{x}_r \in \mathcal{T}_l \quad .$$

$A_l$  is the non-translational component of the deformation and plays a substantial role in describing the non-rigid part of the general transformation  $\Phi_l(\mathbf{x})$ . To be able to fully determine  $A_l$  and  $\mathbf{a}_l$ , a fourth undeformed vertex that is non-planar to with the vertices of  $\mathcal{T}_l$  is required. We therefore choose the fourth vertex to be

$$\mathbf{x}_s = \frac{(\mathbf{v}_q) \times (\mathbf{v}_r)}{\|(\mathbf{v}_q) \times (\mathbf{v}_r)\|^{\frac{1}{2}}} + \mathbf{x}_p \quad , \quad \mathbf{v}_i = \mathbf{x}_i - \mathbf{x}_p \quad \text{and} \quad i \in \{q, r, s\}$$

and obtain a local coordinate frame of  $\mathcal{T}_l$  given by  $\mathcal{A}_l = (\mathbf{x}_p; \mathbf{v}_q, \mathbf{v}_r, \mathbf{v}_s)$  with  $\mathbf{x}_p$  the origin and the  $\mathbf{v}_i$  the basis vectors. Here, the cross-product is scaled by the inverse of the square root of its length in order to obtain a proportional scaling with the triangle edge length. Since our input scans are uniformly sampled, we obtain a reasonable and simple approximation.

Similarly, the deformed vertices  $\tilde{\mathbf{x}}_i$  with  $i \in \{p, q, r, s\}$  form a local coordinate frame  $\tilde{\mathcal{A}}_l = (\tilde{\mathbf{x}}_p; \tilde{\mathbf{v}}_q, \tilde{\mathbf{v}}_r, \tilde{\mathbf{v}}_s)$  with  $\tilde{\mathbf{v}}_i = \tilde{\mathbf{x}}_i - \tilde{\mathbf{x}}_p$  with  $i \in \{q, r, s\}$ . Since  $\mathbf{a}_l = \tilde{\mathbf{x}}_p - A_l \mathbf{x}_p$ , it follows that

$$A = \tilde{V} V^{-1} \quad , \quad V = [\mathbf{v}_q \mathbf{v}_r \mathbf{v}_s] \quad \text{and} \quad \tilde{V} = [\tilde{\mathbf{v}}_q \tilde{\mathbf{v}}_r \tilde{\mathbf{v}}_s] \quad . \quad (2.5)$$

Equation 2.5 shows that the elements of the non-translational components  $A_l$  are linear combinations of the unknown deformed vertices  $\tilde{\mathbf{x}}_i$  and depend on the coordinates of the undeformed vertices  $\mathbf{x}_i$ .

The objective of the shape deformation stage is to compute an affine map  $\Phi_l$  for each triangle  $\mathcal{T}_l$  of a triangle mesh  $\mathcal{M}$  in order to obtain a deformed triangle mesh  $\varphi(\mathcal{M})$ . Since  $\varphi(\mathcal{M})$  is a triangle mesh, we require its shared vertices to be in the same locations. The following constraint ensures *connectivity consistency*:

$$\Phi_j(\mathbf{x}_i) = \Phi_k(\mathbf{x}_i) \quad , \quad \forall i, \forall j, k \in \mathcal{N}_t(i)$$

with  $\mathcal{N}_t(i)$  the indices of triangles adjacent of the vertex of index  $i$ .

Using the deformation model presented above, we can now provide displacements and deformation behaviors as presented in Section 2.1 and 1.2 in terms of

a constrained minimization problem for deforming  $\mathcal{M}$ . More precisely, finding the affine maps  $\Phi_l$  for each triangle can be done by minimizing some energy term  $E(\tilde{\mathbf{x}}_1, \dots, \tilde{\mathbf{x}}_n)$  that depends on the deformed shape  $\mathcal{M}$ . We solve the following minimization for the  $\Phi_l$ :

$$\min_{\Phi_1, \dots, \Phi_m} E(\tilde{\mathbf{x}}_1, \dots, \tilde{\mathbf{x}}_n) \quad \text{subject to} \quad \Phi_j(\mathbf{x}_i) = \Phi_k(\mathbf{x}_i), \quad \forall i, \forall j, k \in \mathcal{N}_t(i);$$

In particular,  $E(\tilde{\mathbf{x}}_1, \dots, \tilde{\mathbf{x}}_n)$  encodes the displacement and deformation assumptions about the scanned object.

When  $E(\tilde{\mathbf{x}}_1, \dots, \tilde{\mathbf{x}}_n)$  depends solely on  $A_l$  (c.f. Equation 2.5), the minimization problem proposed above would be defined in terms of the unknown deformed vertices and the minimization would be over the vertices themselves where the connectivity constraints are implicitly satisfied:

$$\min_{\tilde{\mathbf{x}}_1, \dots, \tilde{\mathbf{x}}_n} E(\tilde{\mathbf{x}}_1, \dots, \tilde{\mathbf{x}}_n) = \|f(\tilde{\mathbf{x}}_1, \dots, \tilde{\mathbf{x}}_n)\|^2 \quad (2.6)$$

with  $f(\tilde{\mathbf{x}}_1, \dots, \tilde{\mathbf{x}}_n)$  a function which squared norm is the energy  $E$ .

Moreover, if  $f(\tilde{\mathbf{x}}_1, \dots, \tilde{\mathbf{x}}_n)$  is linear with  $\tilde{\mathbf{x}}_1, \dots, \tilde{\mathbf{x}}_n$ , the solution of the optimization problem would be the solution of a linear system, and thus efficient to solve. In fact, Equation 2.6 could be rewritten in matrix form:

$$\min_{\tilde{\mathbf{x}}_1, \dots, \tilde{\mathbf{x}}_n} \|\mathbf{c} - M\tilde{\mathbf{y}}\|^2$$

with  $\tilde{\mathbf{y}} = [\tilde{\mathbf{x}}_1^t, \dots, \tilde{\mathbf{x}}_n^t]^t$  a concatenation of all unknown deformed vertices and  $M$  a large, sparse matrix relating  $\tilde{\mathbf{y}}$  to the vector  $\mathbf{c}$ . Further, setting the gradient of the objective function to zero yields the following normal equations:

$$A^t A \tilde{\mathbf{y}} = A^t \mathbf{c}$$

which can be solved efficiently via QR decomposition.

We now specify different objective functions which compute the desired deformations when minimized. In addition, they are linear in  $\tilde{\mathbf{x}}_1, \dots, \tilde{\mathbf{x}}_n$  (c.f. [Sumner & Popović '04]) which dramatically reduces the running time when computing the large number of deformations for the registration of scan sequences.

### Correspondence Constraints

The correspondences determined in Section 2.2 between  $\mathcal{M}_S$  and  $\mathcal{M}_t$  define how the mesh  $\mathcal{M}_S$  should deform. Once the correspondences are pruned, a subset of  $h \leq n$  vertices  $\mathbf{x}_i$  from  $\mathcal{M}_S$  have corresponding points  $\mathbf{c}_i$  which represent the displacements for  $\mathbf{x}_i$ . We note that the  $\mathbf{c}_i$  are not restricted on the mesh  $\mathcal{M}_t$  as it is the case for boundaries. The objective function is given by:

$$E_C(\mathbf{x}_1, \dots, \mathbf{x}_n; \mathbf{c}_1, \dots, \mathbf{c}_h) = \sum_{i=1}^h \|\mathbf{x}_i - \mathbf{c}_i\|^2 \quad .$$

Minimizing this equation forces the corresponding points to be as close as possible when performing the deformation  $\varphi$ .

### Deformation Smoothness Constraints

The assumptions made in Section 1.2 impose the deformations of our object to be smooth in space and time. Thus, the deformations of adjacent triangles should be similar and the deformation itself must be small between two frames. The deformation smoothness constraint in space is given by:

$$E_S(\mathbf{x}_1, \dots, \mathbf{x}_n) = \sum_{j=1}^m \sum_{k \in \mathcal{N}_t(j)} \|A_j - A_k\|_F^2$$

with  $\mathcal{N}_t(j)$  the indices of triangles adjacent of the triangle of index  $j$ . In particular, this term aims at optimizing the smoothness of the change in deformation and not keeping the surface itself smooth. For instance, a global rigid motion of an arbitrary shape would minimize this objective function since the deformations of all triangles are identical.

Similarly the smoothness term in time is defined as:

$$E_I(\mathbf{x}_1, \dots, \mathbf{x}_n) = \sum_{j=1}^m \|A_j - I\|^2 \quad ,$$

which is minimized when all non-translational terms are as close to the identity matrix as possible. We note that this objective function prevents the spatial smoothness term from generating extreme deformations since  $E_S$  tries to optimize the change in shape of adjacent triangles.

### Deformation via Optimization

Combining the correspondence and deformation smoothness constraints  $E_C$ ,  $E_S$ , and  $E_I$ , we obtain the following minimization problem for computing the optimal deformed vertices:

$$\min_{\tilde{\mathbf{x}}_1, \dots, \tilde{\mathbf{x}}_n} E_{\text{tot}}(\mathbf{x}_1, \dots, \mathbf{x}_n; \mathbf{c}_1, \dots, \mathbf{c}_h) \quad (2.7)$$

with

$$E_{\text{tot}} = w_S E_S + w_I E_I + w_C E_C$$

and scalar weights  $w_S$ ,  $w_I$ , and  $w_C$ .  $E_{\text{tot}}$  is a linear combination of objective functions that are linear in  $\tilde{\mathbf{x}}_1, \dots, \tilde{\mathbf{x}}_n$  and is therefore again linear in the deformed vertices. Similar to the research conducted in [Sumner & Popović '04, Allen et al. '03], the weights control the deformation behaviors when iterated deformations are employed for matching shapes. For instance, when  $\mathcal{M}_S$  and  $\mathcal{M}_t$  are initially further apart, we can assume a rigid motion component to be present in the general deformation  $\varphi$ . Therefore, setting a higher value for  $w_S$  at the beginning of the iterations would make the deformation as global as possible, reducing rigid motion components from the overall transformation. After a certain number of iterations (correspondence computation and deformation), when  $\mathcal{M}_S$  has moved closer  $\mathcal{M}_t$ , we increase  $w_C$  and decrease  $w_S$  to better approximate the target mesh.

In order to minimize accumulation errors,  $\varphi(\mathcal{M}_S)$  is recomputed from the original undeformed shape  $\mathcal{M}_S$  after each optimization step of Equation 2.7.

In analogy to registration of rigid shapes, *fractional transformations* can also be considered, as mentioned in [Mitra et al. '04]. More precisely, it makes sense to take smaller steps in the direction of the transformation for each iteration. This is because the correspondence and deformation computations are based on approximants that are only valid locally and no explicit assumption except closeness is made about the initial alignments of the source and target mesh.



# Chapter 3

## Preliminary Results

The primary concern of this preliminary work is to examine the proposed general registration framework presented in Section 2.1 by solving individual sub-problems using simple and well-established techniques.

In order to stretch the limits on what can be achieved, we use methods that make weaker assumptions about the input data than those presented in Section 1.2. For instance correspondence and pruning are achieved simply by using positional information of surface points. No higher order local description of the shape is ever used. Another example is that our deformation model does not enforce isometry. Therefore, the scan of a certain frame can take any shape when a sufficiently large number of deformations is applied to it.

The objective here is to analyze the main issues arising from the proposed methodology, which are exposed in Section 3.1. Implications of the experimental results are discussed in more detail in Section 3.2. All experiments were performed on a 2.16 GHz Intel Core 2 Duo with 2 GB RAM.

### 3.1 Experiments

The evaluation of our experimental results is based on synthetic data as well as on real scans acquired by a recently developed high speed structured light scanner (c.f. [Weise et al. '07]). This section will examine the case with trivial shapes undergoing simple transformations and more complex ones such as an animated cloth. Finally, an example of real scan data undergoing complex deformations is presented where the analysis of the performance of our algorithm w.r.t. stability, tolerance of noise, and outliers will play a substantial role. Equally important, the robustness of the algorithm against ineptly chosen input parameters has to be considered as well.

While most of the algorithms presented in Chapter 2 have parameters that can be determined automatically with simple heuristics (e.g. pruning threshold, deformation weights, etc...), we choose to adjust them manually at this stage of research. The main reason for this is that the performance of the interplay of the individual algorithms are not yet fully understood.

Note that the evaluation of the overall quality of registration methods for rigid objects is usually done by analysing the convergence rate. For the non-rigid case, this is difficult to perform, since, for real data, no correspondence information except estimations is known in advance. For synthetic data however, correspondence can be obtained simply by using the parametrization of a complete 3-D model and acquiring virtual depth maps. Nevertheless, one possible way to examine convergence for real scan data is to use manually selected point-correspondences, which will be fruitful to examine in future work.

### Simple Motions and Deformations

Our first experiment is the registration of a plane undergoing a simple curved motion as shown in Figure 3.1 (a). In addition, the plane is continuously bent as it moves along the motion path. This example has no particular semantic purpose on shape completion of a 3-D model. Instead, it is a simple test to see if the proposed registration scheme behaves as expected for a near-ideal case.

The model has 800 faces and 441 vertices and the input sequence is generated by linear interpolating between a source plane and its deformed target model. In particular, mesh connectivity is preserved during motion and the median edge length is approximately equal to 5 (we use it as a density estimation for our uniformly sampled meshes). We then sample uniformly in time twelve frames as illustrated in Figure 3.1 (b) to obtain the meshes  $\mathcal{M}_1 \dots \mathcal{M}_{12}$ . Accumulating all scans in the same coordinate system as in Figure 3.1 b clarifies the spatial inconsistency when no registration is performed.

We then apply a different number of iterations of the registration algorithm introduced in Equation 2.2. Note that it would be more reliable to use Equation 2.4 although the computation would be more involved. As anticipated, a longer curved surface is obtained for  $\mathcal{M}_{\text{tot}}$  after 11 iterations as shown in Figure 3.1 f. Intermediate results are visualized in the Figures 3.1 (c), (d), and (e) for 3, 5, and 7 iterations, respectively. In particular, we perform for each iteration four registration refinements, i.e. four explicit correspondence, pruning, and deformation steps. For an aggressive pruning we set  $\sigma = 0.1$  instead of estimating the sampling density. To keep the deformation of each step as smooth as possible, we choose  $w_S = 1000$ ,  $w_I = 1$ , and  $w_C = 1$ . Since the correspondences are recomputed in each step, the source scan better adapts itself to the geometry of the target scan as with fractional transformations often an integral part of rigid

ICP (c.f. [Mitra et al. '04]). When the four refinement steps are performed, each pair of consecutive scans are eventually aligned.

In this example, no particular issues are observed and the registration behaves as expected. Moreover, for this simple case, the proposed framework is robust against inadequately chosen input parameters.

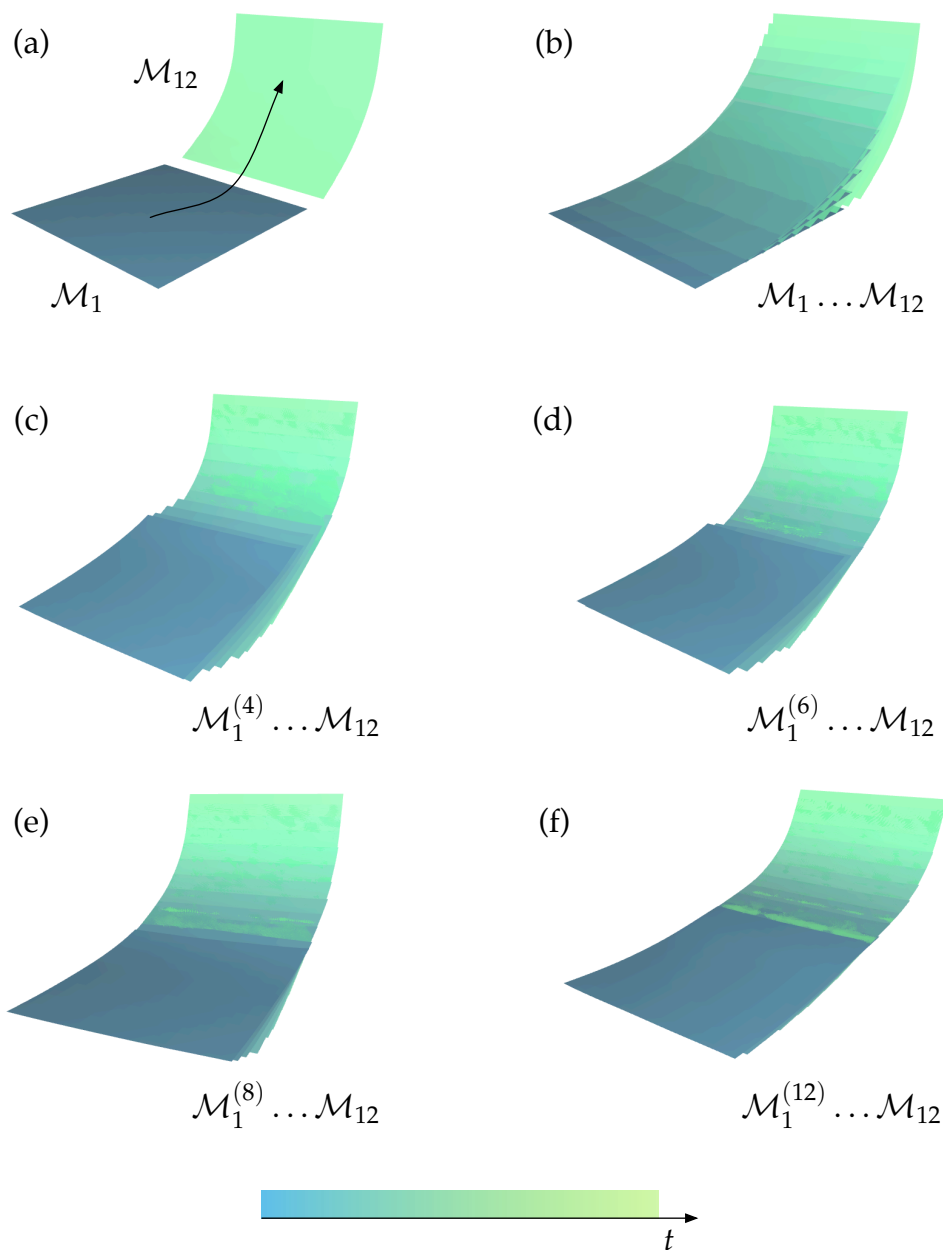


**Figure 3.1:** Data set of a plane undergoing simple motion and deformation. This example examines our approach for a near-ideal case.

### Complex Isometric Deformations

We now look at an example where a quadrangular cloth is deformed by letting it fall onto an invisible sphere. The aim here is to examine how well the registration works on surfaces that undergo large and complex deformations while being isometric and having a low stiffness factor. Because the deformation preserves isometry between edge vertices, a one-to-one point correspondence is explicitly given by the mesh vertices. Ideally, after all iterations of the registration process, the scans from all frames should perfectly match the last one. A deviation from the last scan indicates accumulated inaccuracies of our approach.

A sequence of 20 triangle meshes with each 1024 vertices and 1922 faces is generated with a recent cloth simulation technique described in [Goldenthal et al. '07]. Each frame of the sequence is shown in Figure 3.2 (a). Figure 3.2 (b) displays all frames within a single coordinate system.

We then perform 19 iterations of the registration using the same parameters as the previous experiment from Figure 3.1 except that for the deformation smoothness constraint we set  $w_S = 500$ . Figure 3.2 (c) shows the resulting frames  $\mathcal{M}_1^{(20)} \dots \mathcal{M}_{20}$  simultaneously. Similarly, Figure 3.2 (d), (e), and (f) visualize the frame sequences  $\mathcal{M}_4^{(12)} \dots \mathcal{M}_{20}$ ,  $\mathcal{M}_7^{(20)} \dots \mathcal{M}_{20}$ , and  $\mathcal{M}_{10}^{(20)} \dots \mathcal{M}_{20}$ , respectively. In particular, the set of scans shown in Figure 3.2 (f) is a subset of scans from (e), which itself is a subset of (d) and so on.

This example clarifies the main problem of our approach. In fact, for frames that are close to the target time instance which is 20, in this case the last 10 frames, a reasonable registration can be obtained. However, the further we dissociate in time from the target scan, the less accurate and robust our registration becomes. Therefore only a portion of the frame sequence can be registered correctly, namely those around the target frame.

Figure 3.2 (g) compares the wireframes between the meshes  $\mathcal{M}_6^{(20)}$  and  $\mathcal{M}_{20}$  and (h) between  $\mathcal{M}_{15}^{(20)}$  and  $\mathcal{M}_{20}$ .

We clearly observe that the deformation in Figure 3.2 (g) becomes unstable at some point. This is mainly due to the dominating constrain of the smoothness term in space  $E_S$  over the smoothness term in time  $E_T$  as discussed in Section 2.3. Consequently the surface become stretched and the edges at the mesh boudary become longer.

Note that we decreased the influence of the spatial smoothness term  $E_S$  as we found out that the registration did not manage to align well the corresponding regions with the previous parameter.

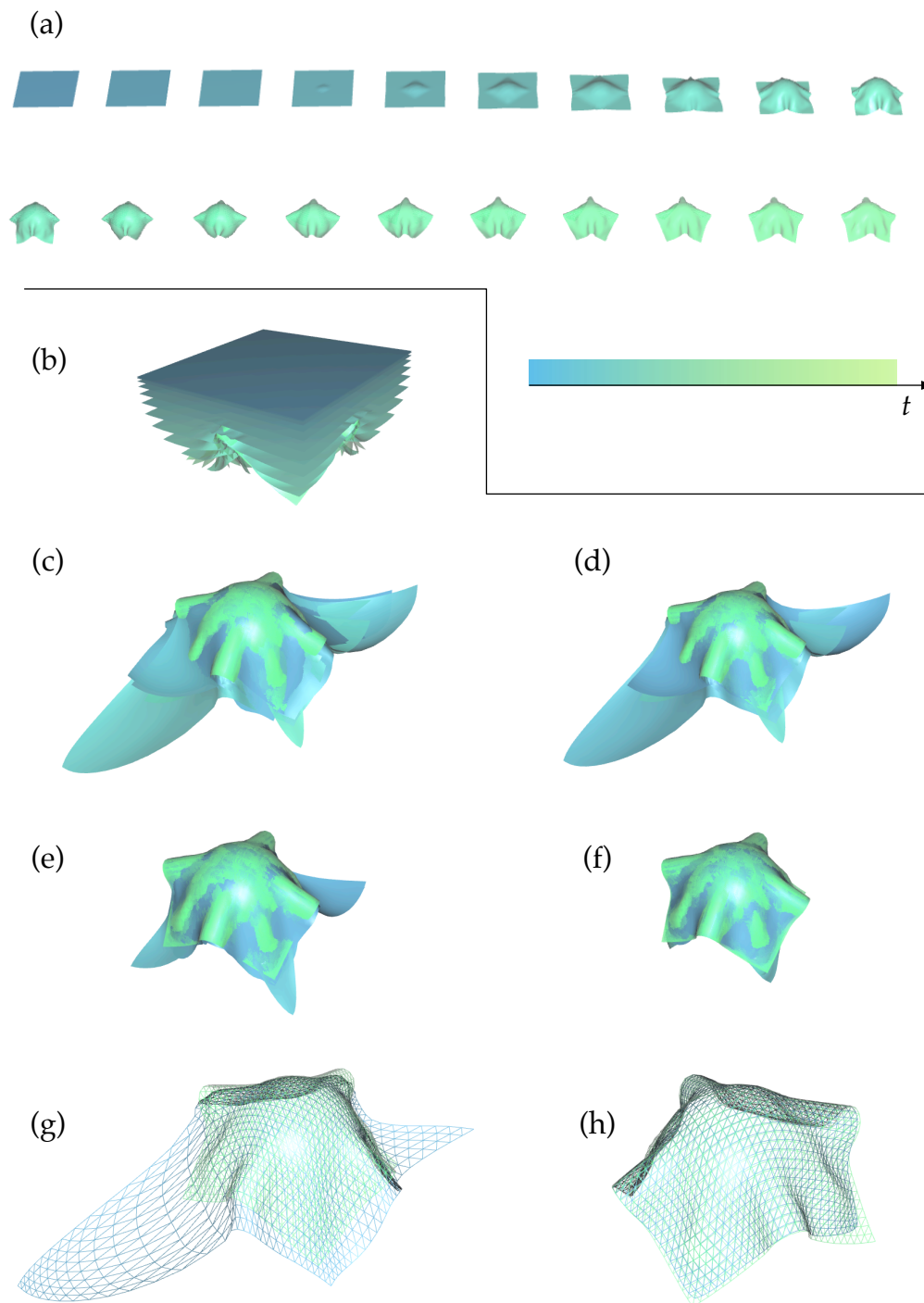


**Figure 3.2:** Data set of a cloth falling onto an invisible sphere. This example examines our registration technique for the case of complex but isometric deformations.

### Real Input Scans

Unless explicitly mentioned, all examples with real scan data in this report are acquisitions captured using a real-time 3-D scanner based on structured light [Weise et al. '07]. The system uses a standard DLP projector and two high speed cameras with a resolution of  $640 \times 480$  pixels. The acquisition method uses a phase-shift pattern and GPU based accelerated processing for solving correspondences of the optical triangulation. Phase discontinuity is overcome using data acquired simultaneously from the two cameras and a motion compensation technique reduces artifacts due to fast motion in the depth direction. The overall shape acquisition rate is between 13 and 15 fps depending on the complexity of the scene. A working space of approximately 1 cubic meter is possible.

Comparing to synthetic input data, the main difference of using real scan data is that artifacts due to hardware limitations are introduced and usually the shape and deformations of the scanned object are more complex (c.f. Section 1.2). Since our ultimate goal is to perform registration of arbitrary scans captured from the real world, we will attempt to explore the performance of our approach on the acquisition of a grasping hand, shown in Figure 3.3 (a). Each captured mesh contains approximately 30 K vertices and 60 K faces and the mesh connectivity varies for each frame. The hand is a non-trivial example, as it exposes different types of deformations simultaneously. For instance, the movement of the fingers represents a mixture of articulated and non-rigid deformation. This is clarified in Figure 3.3 (b) where again we gather all frames into a same coordinate system. Moreover, the amount of rigidity also varies for different locations of the object's surface.

Using the same input parameters as for the first example described in Figure 3.1 except for a stronger influence of the deformation smoothness term  $E_S = 10000$ , we perform 9 iterations of the registration and obtain a very biased result as illustrated in Figure 3.3 (c). However, if we only compute the registration for the last four scans, as shown in Figure 3.3 (d), a reasonable result can be produced, as demonstrated in Figure 3.3 (e). Similar to the animated cloth example in Figure 3.2, our proposed approach is only reliable for frames close to the target ones. Again, the hypothesis is that the method seems to be mainly limited by the accumulation of errors in each iteration. In addition, we note that no registration with integrated scans as presented in Section 2.1 is performed in this example. As a consequence, many corresponding regions do not perfectly align.

An interesting visualization of the deformation behavior is shown in Figure 3.3 (f) where the scans  $\mathcal{M}_1^{(1)}, \mathcal{M}_1^{(5)}, \mathcal{M}_1^{(10)}$  track the progress of deformation of the first acquired scan. Figure 3.3 (g) shows the same visualization for the scans  $\mathcal{M}_6^{(6)}, \mathcal{M}_6^{(8)}, \mathcal{M}_6^{(10)}$  originally acquired at time 6. We see that the shape nicely wraps itself around the shape of the target scan  $\mathcal{M}_{10}$ .

Furthermore, Figure 3.3 (2) (a), (b), (c), and (d) show an incremental visualization of the individual scans from Figure 3.3 (c) added one after the other.

## 3.2 Caveats and Implications

Different scenarios of input data were examined using our registration framework. Our experiments showed that even for rudimentary methods for solving the pairwise correspondence and deformation problems, good results could be produced for frames that are close in time with the target frame. This also means that for small deformations for the scanned object, correspondences based solely on positional informations and general deformation algorithms are relatively well suited. However, for objects that undergo larger deformations, the registration approach becomes unstable and results in unaligned scans, misalignments and drastic deformations. We will see next that the cause of these issues are all related to each other.

### Unaligned Regions

A plausible cause for unaligned scans is that we did not use integrated scan registrations as introduced in Section 2.1 for our experiments. Another source for unaligned regions is produced by using global weights for the deformation smoothness, i.e.  $w_S$  and  $w_I$ , throughout the registration process. As an increased influence of  $w_S$  and  $w_I$  makes the pairwise refinement behave like a fractional transformation, the alignment of shape regions that are too far away might not be complete.

We draw from this observation that an incorporation of integrated scan registration is necessary in order to avoid unaligned regions. In particular, a careful design is advised since the correspondence between non-consecutive scans is even more sensitive to error accumulation. Also, an automatic and more adaptive estimation of the deformation parameters is likely to reduce unaligned regions. In particular, scans that are closer in shape and position should be less constrained by  $E_S$  and  $E_I$ .

### Misalignments

We refer to misalignments as matched regions that are differing from the correct corresponding region after the registration. For consecutive scans, correspondence estimations using our non-rigid ICP-based refinement have proven to be relatively reliable, but still imperfect. Hence, an accumulation of small errors results in inconsistent alignments after multiple iterations of the registration.

As opposed to global rigid registration (c.f. [Gelfand et al. '05, Pulli '99]), solving our problem exclusively with local optimizations is hard since we do not yet possess a clear formulation of an overall error minimization term toward which the algorithm should converge. Moreover, non-rigid deformations are inherently sensitive to incorrect correspondence estimations, which again is not the case for rigid registrations.

At this point, an immediate remedy to this problem seems to be improving the correspondence and pruning stage with more sophisticated local shape matching methods that locally approximate the surface at higher orders. Also, from the temporal coherence assumption between scans that are close in time, we could consider multiple frames in proximity for performing a single registration iteration instead of just a pair of consecutive scans. And since our input scans are affected by noise, perhaps it makes sense to use a target scan for correspondence that is represented at a coarser level (e.g. via smoothing).

In addition, adding more restrictions into the deformation model would increase robustness to accumulated correspondence errors from the registration refinement. As mentioned previously, registration using near-isometric deformations were not investigated in this report. Although an isometric deformation would prevent the shapes from bloating as illustrated in Figure 3.3 (c), undesired creases as known for cloth simulation techniques might appear. Thus, the behavior of a more appropriate and efficient deformation model that includes the assumptions presented in Section 1.2 remains to be investigated.

Another question to answer is under what circumstances each deformation step should be computed from its original shape. This has been briefly addressed at the end of Section 2.3, but has not yet been incorporated into the implementation for our experiments.

### Uncontrolled Drastic Deformations

Drastic deformations were often observed in our experiments (c.f. Figure 3.2 (c), (d), (e), and 3.3 (c)). As seen previously, the main reason for this improper behavior is due to the dominating weights of the spatial smoothness term  $E_S$  over the temporal one  $E_T$ . However, keeping deformation stability under control using this deformation model is difficult since our parameters should be valid globally throughout the registration process for a fully automatic approach.

Other than using a more restrictive deformation model, one possibility would be to integrate a trial an error mechanism which locally increases the temporal deformation term when a drastic deformation is being detected.

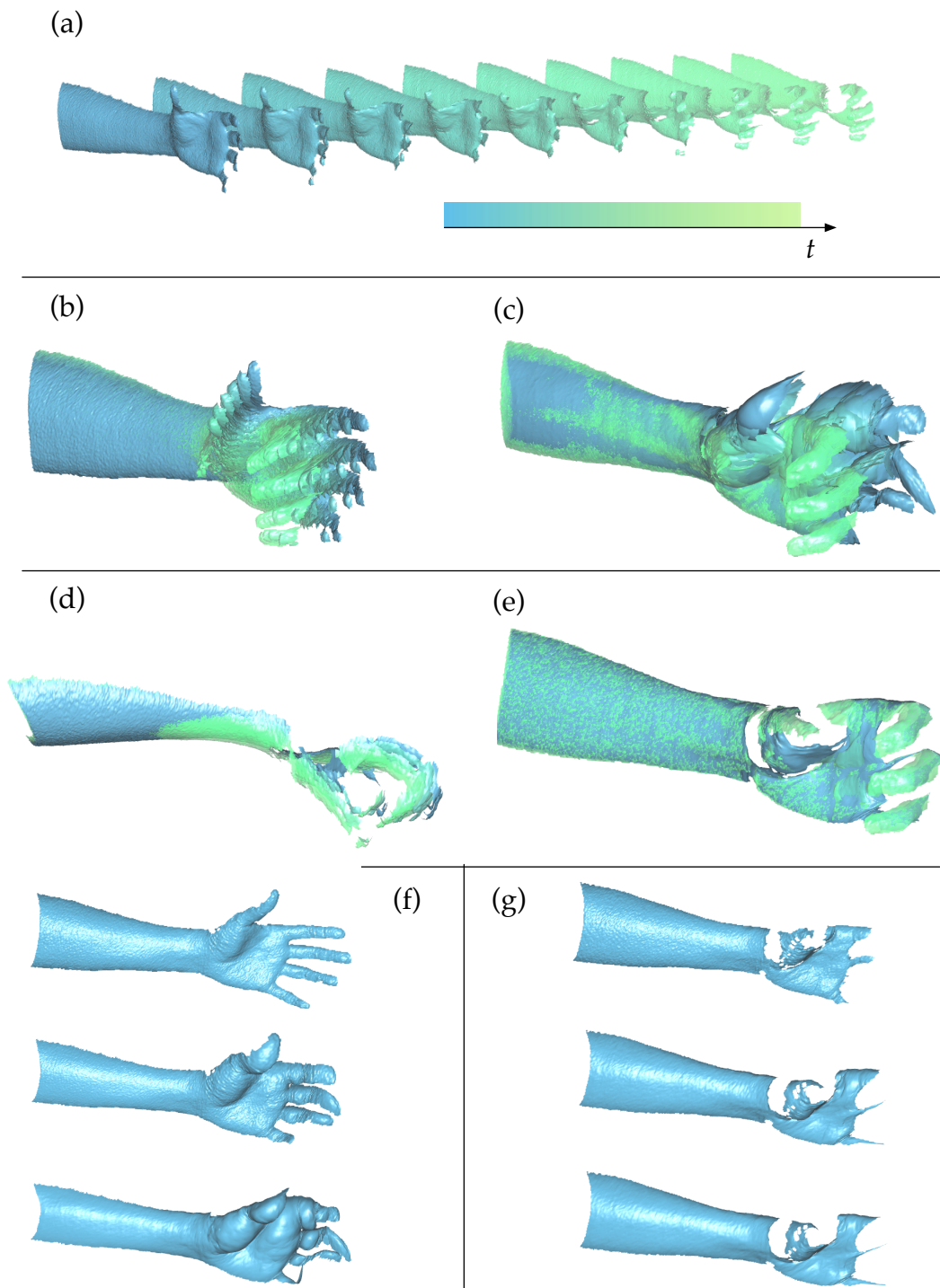


**Figure 3.3:** Data set of grasping hand acquired using a high-speed structured light scanner. This example examines our method for the case of real input data which undergoes complex deformations and is significantly affected by noise, outliers, and acquisition holes.

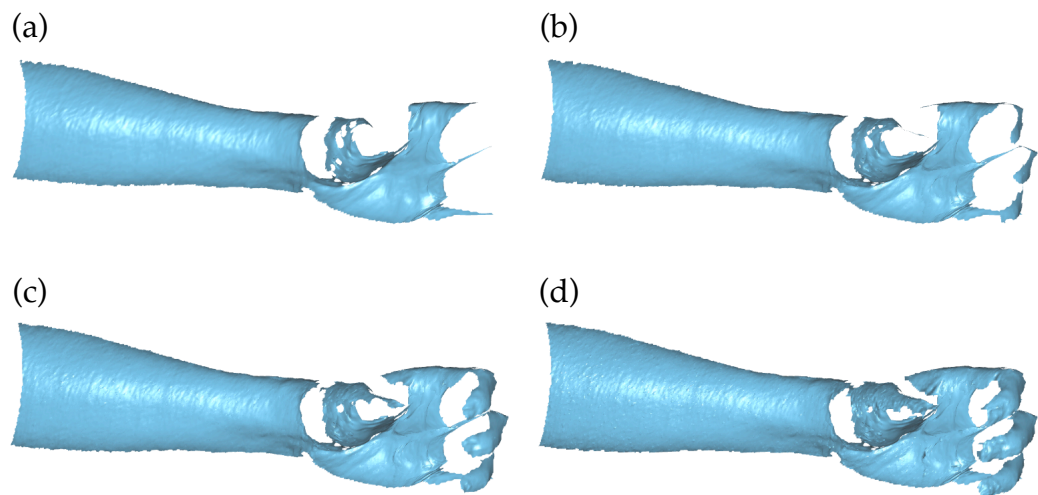


**Figure 3.4:** Incremental visualization of the individual scans of a comparatively successful registration from Figure 3.3 (c).

# Chapter 4

## Summary and Outlook

### 4.1 Research Status

This report provides an analysis of the registration problem from scans of deformable objects captured with a high-speed 3-D scanner. A detailed comparison to other types of scan registration algorithms allowed us to clarify the assumptions to make in our specific setting. Also, it helped us determine well-established techniques upon which our algorithms were built.

The registration scheme for time coherent and deforming scans proposed herein represents a general framework for obtaining the complete object at an arbitrary instance in time. In this work, the focus is to obtain the registration for the time instance of the last acquisition. The method has two iteration loops. The outer loop propagates each scan to the next time instance and the inner loop performs a non-rigid ICP method decoupling the correspondence and the deformation problem.

Both sub-problems were addressed using a general approach where not all assumptions mentioned in Section 1.2 were taken into consideration. In the correspondence stage, we only examined the closest point method and our deformation model is mainly dictated by smoothness constraints about the object. Also, the pruning of correspondences is currently only based on positional information.

Consequently, the resulting registration is only able to perform adequately for near-ideal input data and scans undergoing complex deformations as long as the amount of deformation is small. As expected, our method breaks down for large scale deformations since it does not fully adhere to our imposed assumptions. The main sources of errors and their implications were discussed in detail in Section 3.2, where different strategies for improvement were presented.

One issue that has not been discussed so far, is the cost of the overall computation. There are two main bottlenecks in our approach: the corresponding point computation and the deformation which requires solving a sparse linear system. Although for a pair of scans, the computation time is still reasonable (in the order of several seconds on a modern PC for complex scans), our problem consists of computing multiple registration refinements which again consist of multiple deformations. Furthermore, it is evident that the registration problem we are facing deals with a large amount of high-resolution input scans. Nevertheless, the issue of efficiency will not be handled as a primary objective in this work as we strive to obtain high-quality 3-D reconstructions.

## 4.2 Future Directions

Putting the implications discussed in Section 3.2 into perspective, our preliminary work opens up a whole new line of focus:

- **Accurate Correspondence:**

For the correspondence step in the pairwise refinement, we did not examine the performance of tangent plane projections in our experiments. Since it has been proven to converge faster than the closest point approach for rigid ICP, it might behave similarly for the non-rigid case. Depending on the initial alignments of a pair of scans, the corresponding point might not be located on the target surface point. For this, we might define a termination criterion that consist of repeating the refinement until the distance of all corresponding points that are initially close converge to zero.

Another option for improving correspondence is to consider higher order shape descriptions. For instance normal information or even local curvature approximations can be taken into account in addition to just positional information. An even rougher method would consist of fragmenting a source scan into multiple large patches and rigidly matching each one to the target scan. The displacements of all vertices will then form the pairwise point-to-point correspondences. This way, correspondence would be more attuned to local shape matching based on rigid regions of articulated deformations.

- **Robust Deformation:**

As our experiments confirm, the accumulation of many negligible errors introduced in the individual refinement iterations can cause drastic errors in the resulting registration. They are manifested in disfigured meshes where the edge lengths are likely to change considerably as soon as a cer-

tain number of iterations is attained. We see two immediate possible solutions.

Since the deformation in each iteration is computed from a deformed shape, except for the first iteration, the initial steady state of each acquired scan becomes unrecoverable. One possibility here is to design the registration scheme such that all deformations are computed from the scan's initial shape.

Although this might reduce the amount of accumulated errors, more advanced deformation models that impose stronger restrictions about the behavior of the scanned surface would be more robust. As mentioned earlier, near-isometric deformations might be the next step to explore.

- **Learning Deformation Models:**

So far, our registration method is based on prior assumptions about the deformation model. Consequently, it might not be suitable for the scanned object in question. One solution would be to estimate the parameters of a general deformation model from partial observations of the scene geometry. This also means that additional unknown variables would have to be determined in the optimization routine, which makes the registration problem even more difficult.

However, first steps toward learning deformations from acquisition data have already been proposed recently (c.f. [Allen et al. '06], *anguelov05scape*). In particular, they require a template 3-D model of a complete object.

- **Registration of Articulated Scans:**

Another type of data we did not examine in our experiments is articulated objects with rigid components. This represents a specific subtype of our general registration problem. As opposed to the hand example, the transformation is restricted to multiple rigid motions each belonging to a specific surface region. If we want to keep our general deformation procedure, we could find a way to infer rigid motions and use them for the correspondence. In some way, this is a simplified method for learning deformation models. Techniques for extracting rigidity are studied in research on skinning mesh animations (c.f. [James & Twigg '05]) and partial and approximate symmetry detection (c.f. [Mitra et al. '06]).

- **Multi-view Registration:**

In this work, we focussed on the registration of dynamic objects from a single range sensor for which the working space is approximately 1 cubic meter. When the scanned object is too large (e.g. a human body) so that an important region cannot be seen at all for a significant amount of

capturing period, there would be no way to know what shape this non-acquired region would have during this period. The problem is therefore underdetermined in the general case.

One avenue to make sure most regions are covered during the acquisition would be to combine multiple range scanners acquiring a dynamic object from different perspectives simultaneously. As a result, this might form the beginning of a new registration problem consisting of combining multiple scan sequences that are sparsely distributed in space, but each of them sampling the scene densely in space and time.

# Bibliography

- [Allen et al. '03] Brett Allen, Brian Curless und Zoran Popović. The space of human body shapes: reconstruction and parameterization from range scans. In *SIGGRAPH '03: ACM SIGGRAPH 2003 Papers*, S. 587–594, New York, NY, USA, 2003. ACM Press.
- [Allen et al. '06] Brett Allen, Brian Curless, Zoran Popović und Aaron Hertzmann. Learning a correlated model of identity and pose-dependent body shape variation for real-time synthesis. In *Proceedings of the 2006 ACM SIGGRAPH/Eurographics symposium on Computer animation*, S. 147–156, Aire-la-Ville, Switzerland, 2006. Eurographics Association.
- [Amberg et al. '07] Brian Amberg, Sami Romdhani und Thomas Vetter. Optimal Step Nonrigid ICP Algorithms for Surface Registration. In *IEEE Conference on Computer Vision and Pattern Recognition 2007 (CVPR'07)*, June 2007.
- [Anguelov et al. '04] D. Anguelov, D. Koller, P. Srinivasan, S. Thrun, H.-C. Pang und J. Davis. The correlated correspondence algorithm for unsupervised registration of nonrigid surfaces. In *Advances in Neural Information Processing Systems (NIPS 2004)*, Vancouver, Canada, 2004.
- [Anguelov et al. '05] Dragomir Anguelov, Praveen Srinivasan, Daphne Koller, Sebastian Thrun, Jim Rodgers und James Davis. SCAPE: shape completion and animation of people. *ACM Trans. Graph.*, 24, Nr. 3, S. 408–416, 2005.
- [Bentley '75] Jon Louis Bentley. Multidimensional binary search trees used for associative searching. *Commun. ACM*, 18, Nr. 9, S. 509–517, 1975.
- [Besl & McKay '92] P. J. Besl und N. D. McKay. A method for registration of 3D shapes. *IEEE Transactions on Pattern Analysis and Machine Intelligence*, 14, Nr. 2, S. 239–256, February 1992.
- [Botsch & Kobbelt '04] M. Botsch und L. Kobbelt. A remeshing approach to multiresolution modeling, 2004.

- [Botsch & Sorkine '07] Mario Botsch und Olga Sorkine. On linear variational surface deformation methods. *IEEE Transactions on Visualization and Computer Graphics*, 2007. To appear.
- [Brown & Rusinkiewicz '04] Benedict Brown und Szymon Rusinkiewicz. Non-Rigid Range-Scan Alignment Using Thin-Plate Splines. In *Symposium on 3D Data Processing, Visualization, and Transmission*, 2004.
- [Brown & Rusinkiewicz '07] Benedict Brown und Szymon Rusinkiewicz. Global Non-Rigid Alignment of 3-D Scans. *ACM Transactions on Graphics (Proc. SIGGRAPH)*, 26, Nr. 3, August 2007.
- [Chen & Medioni '92] Yang Chen und Gérard Medioni. Object modelling by registration of multiple range images. *Image Vision Comput.*, 10, Nr. 3, S. 145–155, 1992.
- [Chen et al. '98] Chu-Song Chen, Yi-Ping Hung und Jen-Bo Cheng. A Fast Automatic Method for Registration of Partially-Overlapping Range Images. In *ICCV '98: Proceedings of the Sixth International Conference on Computer Vision*, S. 242, Washington, DC, USA, 1998. IEEE Computer Society.
- [Chui & Rangarajan '00] H. Chui und A. Rangarajan. A new point matching algorithm for non-rigid registration, 2000.
- [Gelfand et al. '03] Natasha Gelfand, Leslie Ikemoto, Szymon Rusinkiewicz und Marc Levoy. Geometrically Stable Sampling for the ICP Algorithm. In *Fourth International Conference on 3D Digital Imaging and Modeling (3DIM)*, Oktober 2003.
- [Gelfand et al. '05] Natasha Gelfand, Niloy J. Mitra, Leonidas J. Guibas und Helmut Pottmann. Robust Global Registration. In *Symposium on Geometry Processing*, S. 197–206, 2005.
- [Goldenthal et al. '07] Rony Goldenthal, David Harmon, Raanan Fattal, Michel Bercovier und Eitan Grinspun. Efficient Simulation of Inextensible Cloth. *ACM Transactions on Graphics (Proceedings of SIGGRAPH 2007)*, 26, Nr. 3, 2007.
- [Hähnel et al. '03] D. Hähnel, S. Thrun und W. Burgard. An Extension of the ICP Algorithm for Modeling Nonrigid Objects with Mobile Robots. In *Proceedings of the Sixteenth International Joint Conference on Artificial Intelligence (IJCAI)*, Acapulco, Mexico, 2003. IJCAI.
- [Huber & Hebert '01] Daniel F. Huber und Martial Hebert. Fully Automatic Registration of Multiple 3D Data Sets. In *IEEE Computer Society Workshop on Computer Vision Beyond the Visible Spectrum (CVBVS 2001)*, Dezember 2001.

- [James & Twigg '05] Doug L. James und Christopher D. Twigg. Skinning mesh animations. In *SIGGRAPH '05: ACM SIGGRAPH 2005 Papers*, S. 399–407, New York, NY, USA, 2005. ACM Press.
- [Johnson & Hebert '97] A. Johnson und M. Hebert. Surface registration by matching oriented points, 1997.
- [Koninckx et al. '05] Thomas P. Koninckx, Pieter Peers, Philip Dutre und Luc Van Gool. Scene-Adapted Structured Light. In *CVPR '05: Proceedings of the 2005 IEEE Computer Society Conference on Computer Vision and Pattern Recognition (CVPR'05) - Volume 2*, S. 611–618, Washington, DC, USA, 2005. IEEE Computer Society.
- [Levoy et al. '00] Marc Levoy, Kari Pulli, Brian Curless, Szymon Rusinkiewicz, David Koller, Lucas Pereira, Matt Ginzton, Sean Anderson, James Davis, Jeremy Ginsberg, Jonathan Shade und Duane Fulk. The Digital Michelangelo Project: 3D Scanning of Large Statues. In Kurt Akeley (Hrsg.), *Siggraph 2000, Computer Graphics Proceedings*, S. 131–144. ACM Press / ACM SIGGRAPH / Addison Wesley Longman, 2000.
- [Li et al. '06] Hao Li, Raphael Straub und Hartmut Prautzsch. Structured Light Based Reconstruction Under Local Spatial Coherence Assumption. In *Symposium on 3D Data Processing, Visualization, and Transmission*, June 2006.
- [Li '05] Hao Li. Rekonstruktion farbiger Objekte aus strukturiert beleuchteten Ansichten. Technical report, Universität Karlsruhe (TH), June 2005.
- [Mitra & Nguyen '03] Niloy J. Mitra und An Nguyen. Estimating surface normals in noisy point cloud data. In *SCG '03: Proceedings of the nineteenth annual symposium on Computational geometry*, S. 322–328, New York, NY, USA, 2003. ACM Press.
- [Mitra et al. '04] Niloy J. Mitra, Natasha Gelfand, Helmut Pottmann und Leonidas Guibas. Registration of point cloud data from a geometric optimization perspective. In *SGP '04: Proceedings of the 2004 Eurographics/ACM SIGGRAPH symposium on Geometry processing*, S. 22–31, New York, NY, USA, 2004. ACM Press.
- [Mitra et al. '06] Niloy J. Mitra, Leonidas J. Guibas und Mark Pauly. Partial and approximate symmetry detection for 3D geometry. In *SIGGRAPH '06: ACM SIGGRAPH 2006 Papers*, S. 560–568, New York, NY, USA, 2006. ACM Press.

- [Mitra et al. '07a] N. J. Mitra, S. Flöry, M. Ovsjanikov, N. Gelfand, L. Guibas und H. Pottmann. Dynamic Geometry Registration. In *Symposium on Geometry Processing*, 2007.
- [Mitra et al. '07b] N. J. Mitra, L. Guibas und M. Pauly. Symmetrization. In *ACM Transactions on Graphics*, 2007.
- [Pauly et al. '05] Mark Pauly, Niloy J. Mitra, Joachim Giesen, Markus H. Gross und Leonidas J. Guibas. Example-Based 3D Scan Completion. In *Symposium on Geometry Processing*, S. 23–32, 2005.
- [Pottmann & Hofer '03] H. Pottmann und M. Hofer. Geometry of the squared distance function to curves and surfaces. In H.-C. Hege und K. Polthier (Hrsg.), *Visualization and Mathematics III*, S. 223–244. Springer, 2003.
- [Pottmann et al. '04] H. Pottmann, S. Leopoldseder und M. Hofer. Registration without ICP. *Computer Vision and Image Understanding*, 95, Nr. 1, S. 54–71, 2004.
- [Pottmann et al. '06] Helmut Pottmann, Qi-Xing Huang, Yong-Liang Yang und Shi-Min Hu. Geometry and Convergence Analysis of Algorithms for Registration of 3D Shapes. *Int. J. Comput. Vision*, 67, Nr. 3, S. 277–296, 2006.
- [Pulli '99] K. Pulli. Multiview Registration for Large Data Sets, 1999.
- [Roth '99] G. Roth. Registering two overlapping range images, 1999.
- [Rusinkiewicz & Levoy '01] Szymon Rusinkiewicz und Marc Levoy. Efficient Variants of the ICP Algorithm. In *Proceedings of the Third Intl. Conf. on 3D Digital Imaging and Modeling*, S. 145–152, 2001.
- [Rusinkiewicz et al. '02] Szymon Rusinkiewicz, Olaf Hall-Holt und Marc Levoy. Real-time 3D model acquisition. In *SIGGRAPH '02: Proceedings of the 29th annual conference on Computer graphics and interactive techniques*, S. 438–446, New York, NY, USA, 2002. ACM Press.
- [Stoddart & Hilton '96] A. Stoddart und A. Hilton. Registration of multiple point sets, 1996.
- [Sumner & Popović '04] Robert W. Sumner und Jovan Popović. Deformation transfer for triangle meshes. In *SIGGRAPH '04: ACM SIGGRAPH 2004 Papers*, S. 399–405, New York, NY, USA, 2004. ACM Press.
- [Weise et al. '07] Thibaut Weise, Bastian Leibe und Luc Van Gool. Fast 3D Scanning With Automatic Motion Compensation. In *IEEE Conference on Computer Vision and Pattern Recognition 2007 (CVPR'07)*, June 2007.

- [Weyrich et al. '04] Tim Weyrich, Mark Pauly, Richard Keiser, Simon Heizle, Sascha Scandella und Markus Gross. Post-processing of Scanned 3D Surface Data. In *SGP '04: Proceedings of the 2004 Eurographics/ACM SIGGRAPH symposium on Geometry processing*, S. 85–94, New York, NY, USA, 2004. ACM Press.
- [Zhang et al. '02] Li Zhang, Brian Curless und Steven M. Seitz. Rapid Shape Acquisition Using Color Structured Light and Multi-pass Dynamic Programming. In *The 1st IEEE International Symposium on 3D Data Processing, Visualization, and Transmission*, S. 24–36, June 2002.
- [Zhang et al. '06] Song Zhang, Dale Royer und Shing-Tung Yau. High-resolution, real-time-geometry video acquisition system. In *SIGGRAPH '06: ACM SIGGRAPH 2006 Emerging technologies*, S. 14, New York, NY, USA, 2006. ACM Press.

